University of South Carolina
Scholar Commons

Theses and Dissertations

2016

Investigation And Development Of Friction Stir Welding Process For Unreinforced Polyphenylene Sulfide And Reinforced Polyetheretherketone

Hossain Ahmed
University of South Carolina

Follow this and additional works at: http://scholarcommons.sc.edu/etd

 Part of the Aerospace Engineering Commons

Recommended Citation

Ahmed, H.(2016). *Investigation And Development Of Friction Stir Welding Process For Unreinforced Polyphenylene Sulfide And Reinforced Polyetheretherketone.* (Master's thesis). Retrieved from http://scholarcommons.sc.edu/etd/3810

This Open Access Thesis is brought to you for free and open access by Scholar Commons. It has been accepted for inclusion in Theses and Dissertations by an authorized administrator of Scholar Commons. For more information, please contact SCHOLARC@mailbox.sc.edu.

INVESTIGATION AND DEVELOPMENT OF FRICTION STIR WELDING PROCESS FOR UNREINFORCED POLYPHENYLENE SULFIDE AND REINFORCED POLYETHERETHERKETONE

by

Hossain Ahmed

Bachelor of Science
Bangladesh University of Engineering and Technology, 2004

Master of Business Administration
University of Dhaka, 2014

Submitted in Partial Fulfillment of the Requirements

For the Degree of Master of Science in

Aerospace Engineering

College of Engineering and Computing

University of South Carolina

2016

Accepted by:

Michael Van Tooren, Director of Thesis

A.P. Reynolds, Reader

Ramy Harik, Reader

Addis Kidane, Reader

Cheryl L. Addy, Vice Provost and Dean of the Graduate School

© Copyright by Hossain Ahmed, 2016
All Rights Reserved.

DEDICATION

This work is dedicated to my parents: Skm Hasina Begum and Md. Rafiqul Islam.

ACKNOWLEDGEMENTS

I would like to express deep gratitude and thanks to my advisor Dr. Michael Van Tooren, professor and director aerospace studies, University of South Carolina for his guidance, invaluable suggestions, constructive criticisms and sharing his knowledge throughout this work. It has been a great privilege and honor for me to work with him. I would like to express my gratitude to my co-advisor Dr. Ramy Harik for his guidance in my progress. I would also like to thank Dr. A.P. Reynolds and Dr. Addis Kidane for their precious advice in this research and kindly agreeing to officially serve as the readers. I also thank all the staff members of McNair Center for Aerospace Innovation and Research, especially Burton Rhodes, who helped me prepare laboratory equipment from the very beginning of this research. A special thanks to undergraduate students Jonathan K. Justice, Aaron Vincent, Grayson Smith, Adam Baton and Rudd Rachael who worked with me in the labs. I appreciate my fellow graduate students, especially Max Boozer and Akhter Hossain who helped me along the way. Finally, I would like to thank my parents, my wife and kids for their support and encouragements to achieve this goal.

ABSTRACT

The joining of thermoplastics through welding, a specific form of fusion bonding, offers numerous advantages over mechanical joining. It eliminates the use of costly fasteners and has only a limited effect on the strength of the parts being joined since it does not require the introduction of holes and loading pins, and it does not create significant stress concentrations. A specific form of welding, Friction Stir Welding, was investigated for the creation of butt joints of unreinforced polyphenylene sulfide (PPS) and short carbon fiber reinforced polyetheretherketone (PEEK) plates. Friction stir welding requires a rotating pin, a shoulder arrangement, relative movement between the tool and the weld piece and a clamping mechanism to hold the weld piece in place. Analytical models and experimental results show that the heat generated by the FSW tool is insufficient to produce the heat required to weld thermoplastic materials which makes FSW of polymers different from FSW of metals. A second heat source is required for preheating the thermoplastic parts prior to welding. A resistance type surface heater was placed at the bottom of two identical weld pieces for the experiments. Two types of shoulder design i.e. a rotating shoulder and a stationary shoulder were developed. Taguchi's Design of Experiment method was utilized to investigate the welding process, where duration of heating, process temperature, tool rotational speed and tool traverse speed were used as the welding parameters. The quality of the welding process was assumed to be indicated by the weld strength. DoE revealed that one of the process parameters, tool traverse speed, had significant influence on the tensile strength of PPS

samples. While PPS sample showed relatively lower tensile strength with higher traverse speed, short carbon fiber reinforced PEEK samples had higher tensile strength with higher traverse speeds.

In addition to tensile tests on dog bone shaped specimen, fracture toughness tests were performed for both PPS and PEEK samples to identify the fracture toughness of these materials. Presence of un-welded section in the welded specimen due to the setup of the experiments yielded notched tensile strengths during the tensile test process. With the help of fracture toughness values of these materials, notched tensile strengths of the welded samples were compared with the notched tensile strengths or residual tensile strengths of the base materials. In this study, residual joint efficiency of PEEK samples was found higher than that of PPS samples. Additionally, notched tensile strengths of the welded samples were compared with un-notched tensile strengths of the materials. The notched tensile strengths of PPS and PEEK were found about 80% and 75% of the respective base materials. Micrographs of PEEK samples showed the presence of more voids and cracks in the weld line compared to the un-welded samples.

In this study, continuous friction stir welding process has been developed for butt joining of unreinforced PPS and short carbon fiber reinforced PEEK. The process parameters and the experimental setup can be utilized to investigate the weldability of different types of thermoplastic composites and various types of joint configurations.

TABLE OF CONTENTS

LIST OF TABLES

LIST OF FIGURES

LIST OF SYMBOLS

A	Contact surface
ω	Angular velocity.
P_m	Mechanical power delivered by the milling machine.
η	Heat transformation efficiency.
F_P	Resultant tangential force at the perimeter.
F_{tp}	Ttangential force at the perimeter of the pin,
F_{ts}	Tangential force at the perimeter of the shoulder
r	Radial distance of the perimeter force
r_o	Pin radius
r_s	Shoulder radius
q	Heat flux
Q_{pt}	The amount of heat produced at pin tip
Q_{po}	The amount of heat produced at pin outer surface
Q_{ss}	The amount of heat produced at shoulder bottom surface
τ_{yield}	Shear yield strength.
τ	Contact shear stress
Tg	Glass transition temperature
Tm	Melting temperature
μ	Friction coefficient

LIST OF ABBREVIATIONS

ANOVA ..... Analysis of Variance

ASTM ..... American Society for Testing and Materials

CNC ..... Computer Numerical Controlled

DOF ..... Degree of Freedom

FSW ..... Friction Stir Welding

HAZ ..... Heat Affected Zone

MTS ..... Material Testing System

PPS ..... Polyphenylene sulfide

PEEK ..... Poly Ether Ether Ketone

SPSS ..... Statistical Package for Social Science

TMAZ ..... Thermo-Mechanically Affected Zone

CHAPTER 1

INTRODUCTION

Significant advances in thermoplastic composite materials make them effective for numerous industrial applications; specifically, in the Aerospace industry. The latest advancement show that the thermoplastics can be used in more, increasingly large primary structure components [1]. Fokker manufactures the horizontal tail of the in-development Agusta Westland AW169 medium twin helicopter and the in-service Gulfstream G650 business jets have their rudder and elevators made of thermoplastics [2] [3].

Composites are highly sought after for their high specific strength and stiffness as well as durability in corrosive and fatiguing environments. Thermoplastic composites are playing a vital role in the development of primary and secondary structures in commercial and military aircrafts. Many companies have developed materials and processes that enable to produce continuous fiber reinforced advanced matrices. Numerous advantages made thermoplastic materials attractive in the aerospace industry. They offer unlimited shelf life, high toughness, short process cycle times and reformability, which allows a level of integrated manufacture that is unachievable with thermoset based composites.

The engineering thermoplastics came on the market in the 1980's. The most promising thermoplastics in aerospace applications, such as polyphenylene sulfide (PPS), polyetherimide (PEI) and polyetheretherketone (PEEK), require relatively high

processing temperatures. The production of parts and assemblies of thermoplastic composites differ significantly from their thermoset counterparts.

In industrial applications, proper assembly of composite parts is a key point for the integrity of the primary and secondary structural assemblies. Joining methods for similar and dissimilar thermoplastics are the key for efficient manufacturing [4]. In many cases, methods of mechanical fastening may lead to the risk of damaging the matrix as well as the fibers in the composite material. Drilling and fastening are slow, failure sensitive and expensive [5]. Joining of thermoplastic composites can be done based on fusion bonding techniques instead of drilling and fastening. Some of the fusion welding techniques are ultrasonic welding, induction welding, resistance welding, rotational welding and autoclave based integral consolidation. Fusion bonding or fusion welding is a generic term for joining or welding processes that rely on several factors including melting of base materials of similar compositions, their melting points, applied pressure and time. Due to the high-temperature phase transitions which are the integral part of these processes, a heat-affected zone is created around the joint line. Most of the fusion bonding techniques involves heating and melting the polymer on the bond surfaces of the components and then pressing these surfaces together for polymer solidification and consolidation. A new alternative bonding technique is friction stir welding [6] [7]. It was initially developed by Wayne Thomas at The Welding Institute (TWI) in 1991 for joining metals. It overcomes many of the problems associated with traditional joining techniques. FSW is a solid-state process which produces welds of high quality in difficult-to-weld materials such as aluminum, titanium and their alloys. Inspired by the success of joining metals, researchers are interested to join polymer based products utilizing FSW.

Although successfully applied for unreinforced polymers [8] [9] [10], the application for continuous fiber reinforced thermoplastics is far from trivial. The development of friction stir welding process for specific unreinforced polymers and short fiber reinforced polymers is the goal of this research.

Advantages of FSW lie in the fact that it takes place below the melting point of the material and has the ability to join thermoplastics that are difficult to fusion weld with existing technology. In addition, this process is highly adaptable for automation and robotic use [11] [12]. Some other advantages of FSW include low energy consumption, little joint preparation, no fumes during process operation and pollution associated with most fusion welding techniques [7].

Recently researchers showed interest in FSW of unreinforced thermoplastics [13]. The influence of different process parameters on the joint strength has been analyzed for friction stir spot welding of unreinforced polycarbonate sheets [14] and high density polypropylene [15]. Many researchers worked on microstructure and mechanical properties of friction stirred welded materials [16] [17]. Seth et al. [18] analyzed the mechanical and microstructure properties of friction stir welded polypropylene sheets using a hot shoe method and determined process parameters to achieve minimal disruption of the polymer's microstructure. They hypothesized that the welds should be made at a low translational speed, high shoe temperature, long pressure time and large pin diameter. Panneerselvam et al. [10] joined Nylon 6 plates by FSW with a threaded pin. Pirizadeh et al. [19] developed a 'self-reacting tool' to eliminate the root defect of the welded thermoplastics parts, and hence enhanced the tensile strength of the work piece. Saeedy and Givi [20]investigated the effects of various critical parameters of FSW

such as tool rotational speed, welding speed and tool attack angle on polyethylene and explained the reasons for lower tensile strength of welded parts. Arici and Sinmaz [21] claimed the elimination of root defect by introducing double passes of the welding tool during FSW of polyethylene [21]. But in many cases, researchers concluded the achievement of a good joint is a challenging task [14] [22]. The friction in FSW generates thermal energy and stirring creates relocation of materials. FSW of thermoplastic composites is a complex process including friction, cohesion, adhesion, deformation, recrystallization, consolidation, blending and migration of multi-phase/material blends [23] [24]. In this study, a continuous friction stir welded butt joining process is described for unreinforced PPS. The technology is not suitable to perform continuous FSW of continuous fiber reinforced composites. This study also analyzes the weldability of short fiber reinforced polyether ether ketone (PEEK). It is anticipated that the process requires subtle control over process parameters.

1.1 Research Goal

The development of friction stir welding process for unreinforced PPS and short carbon fiber reinforced PEEK is the goal of this research.

1.2 Research Objectives

A. Development of heat generation model for FSW of thermoplastic polymers.

B. Development of FSW method for unreinforced polyphenylene sulfide (PPS) and Short carbon fiber reinforced polyether ether ketone (PEEK).

1.3 Terminology Used in Friction Stir Welding Process

Friction stir welding is defined as ‘a method for joining two or more workpieces where a tool, moving in a cyclic manner relative to the workpieces, enters the joint

region, locally plasticizes it and moves along the interface thus causing a solid state joint between the workpieces' [25]. In order to avoid confusion and duplication, TWI proposed an initial basic terminology at an early stage of the development of the FSW [7] [25]. Some of the terminologies relevant to this study are appended below:

FSW Tool: The whole of the rotating device between the machine spindle and the workpiece is referred to as the 'tool'. This is the rotating component designed to generate heat by rubbing in contact with the workpiece.

Rotating Shoulder: As the name refers, part of the FSW tool that rotates with the rotation of the spindle and puts required force on the workpiece is the rotating shoulder. The rotating shoulder has the ability to generate heat during the welding process.

Stationary Shoulder: Part of the FSW tool that does not rotate with rotation of the spindle but applies sufficient force on the workpiece is referred to as the stationary shoulder.

Heat Affected Zone (HAZ): The area that is affected only by heat and where no macro plastic deformation is observed is known as HAZ.

Thermo-Mechanically Affected Zone (TMAZ): The area that is affected by both heat and deformation is referred to as TMAZ.

Advancing Side: The side of the weld where the local velocity of the tool has the same direction as the tool traversing direction is called the advancing side.

Retreating Side: The side of the weld where the local velocity of the tool has the opposite direction of the tool traversing direction is called the retreating side.

CHAPTER 2

HEAT GENERATION DURING FRICTION STIR WELDING PROCESS

2.1 Background

Heat generation process in friction stir welding process involves friction and deformation of welding materials. In literature, heat generation process for FSW of metals, particularly for Aluminum, is found widely [23] [26]. In this study, heat generation process has been developed for thermoplastic polymers. To develop this process, the FSW process has been analyzed and a mathematical formulation has been derived.

2.2 Friction Stir Welding Process Description

The FSW process usually takes place under several phases. Depending upon the heat generation process, FSW of thermoplastic can be divided into five phases: i) Plunging, ii) Initial dwelling, iii) Welding, iv) Final dwelling, and v) Pulling out [24] (Figure 2.1).

Plunging phase: In this phase, FSW tool moves downward and makes contact with the weld pieces while rotating (Figure 2.1 (i)). The tool removes material and makes a hole on to the piece until it reaches to desired depth. If a hole is made to the weld pieces prior to this phase, no vertical force is required. In this study, no hole was made prior to this phase and, therefore, vertical force was required to make an introductory hole.

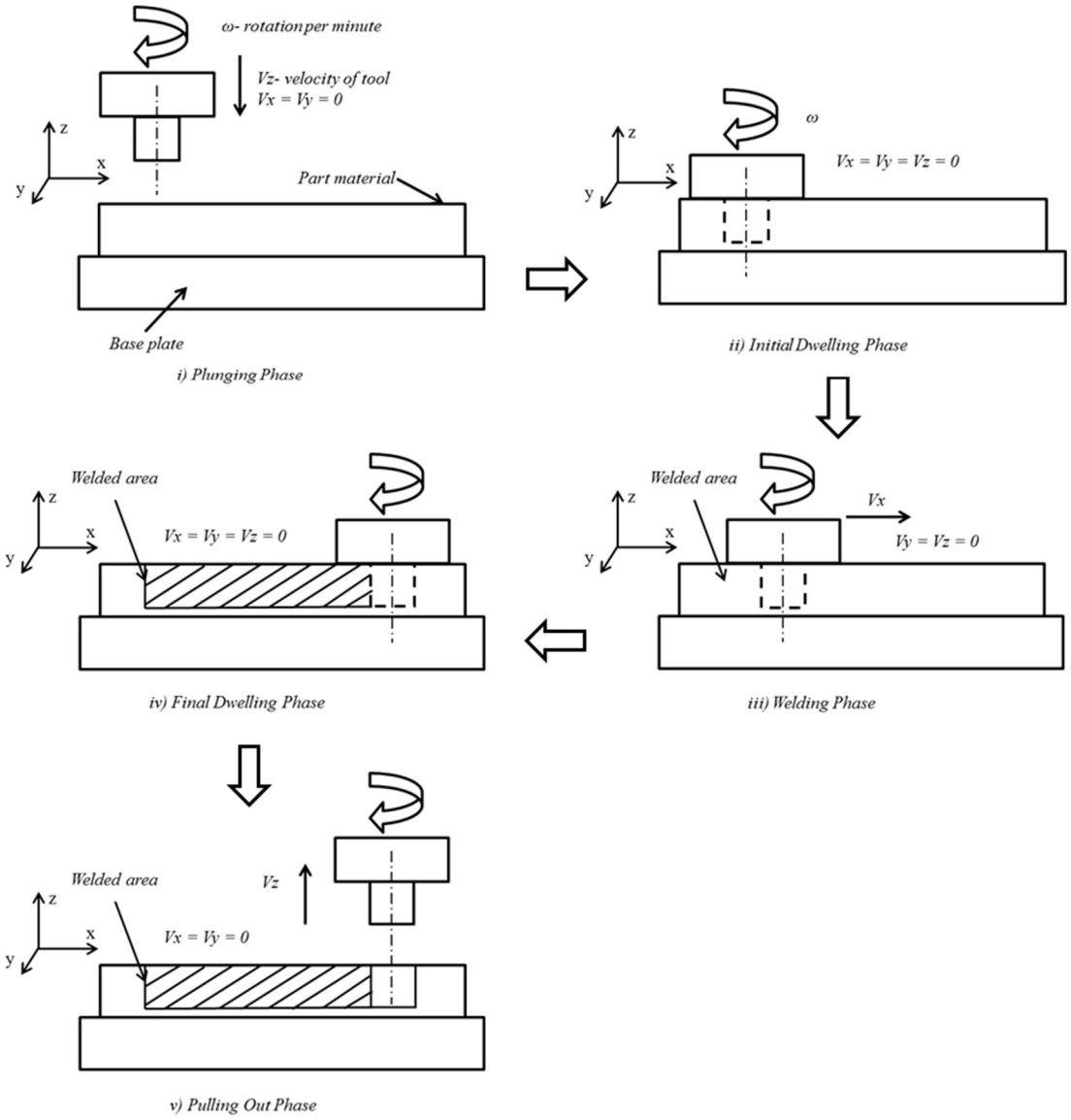

Figure 2.1: Different phases of Friction Stir Welding

Initial dwelling phase: The plunge phase is followed by the dwell phase, where the tool stays steady (no traverse motion) to the welding pieces but still constantly rotating (Figure 2.1 (ii)). The mechanical interactions produce heat by frictional forces. This heat is created by the tool rotating with respect to the stationary work piece which is in contact with the workpiece. The produced heat is dissipated into the surrounding

material. This causes a rise in the temperature of the welding pieces. If the temperature of the thermoplastic rises beyond the glass transition temperature, softening occurs in the surrounding materials.

Welding Phase: At this point, the welding process is initiated by moving the tool and the work piece relative to each other, traversal along the joint line (Figure 2.1 (iii)). This phase is continued to be processed until a planned distance is achieved.

Final dwelling phase: After the welding phase, the traversal movement between the tool and the weld pieces is ceased while the welding tool is still rotating (Figure 2.1 (iv)). This is the third phase or the final dwelling phase. This phase can be avoided if the tool leaves the weld piece while traversing.

Pulling out phase: This is the final phase where the tool is pulled out from the weld piece (Figure 2.1 (v)).

All these phases generate heat utilizing the friction between the contacting surfaces of the tool and the specimen. However, the heat generated during the pulling out phase does not contribute to the joining but is required to complete the welding process. This leaves a hole in the work piece, which is unavoidable, unless the welding process continues to and beyond the edge of the workpiece.

2.3 Heat Generating Contact Surfaces

Different parts of the welding tool and the work piece will remain in contact in different phases. The number of contact surfaces and welding process parameters, such as tool rotational speed, translational speed, axial and transverse force, determine the total heat generation during the process [23] [27] [28] [29]. Figure 2.2 shows the basic

geometry of a welding tool, which consists of a cylindrical shoulder and a cylindrical pin (smaller diameter than shoulder). The shoulder and the pin may have relative movement between them. Depending upon the relative movement of the shoulder, two types of shoulder can be designed: stationary shoulder and rotating shoulder [30]. The tool's pin outer surface is normally threaded which is used to generate sufficient friction and stir the material [26].

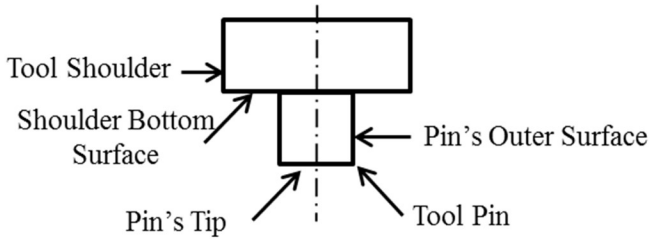

Figure 2.2: Basic tool geometry

During the plunging phase, the pin's bottom surface makes contact with the weld piece and generates heat. As the pin goes down, the side surface of the pin, which has more surface area, makes contact with the weld piece and a significant amount of heat is generated. In this phase, depth of contact increases from 0 to the height of the pin. At the end of the plunging phase, the dwelling phase starts when the shoulder's bottom surface is in contact with the top surface of the weld piece. In the welding phase, all the mentioned surfaces remain in contact with the weld piece while the tool pin's side surface creates normal and shear stress in the weld piece as it moves along the joint line. During the final dwelling phase, the tool pin's side surface, its tip surface and the tool shoulder's bottom surface remain in contact with the weld piece.

2.4 Heat Generation in FSW Process

In friction stir welding, the welding tool penetrates into the base material (Figure 2.3). Because of the rotation of the tool, the base materials are stirred, deformed and welded with each other. During this process, an increase in temperature is observed between the base material and the welding tool, which is due to the influence of rotational and translational motion of the tool. This increase in temperature is an absolute result of heat generation caused by frictional and deformational contact that takes place during the welding process. Figure 2.3 shows a diagram with the basics of the friction stir welding (FSW) process.

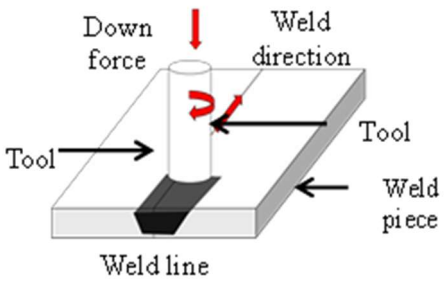

Figure 2.3: Basic process in Friction Stir Welding

Thermal energy generation takes place by transforming mechanical energy into heat [31]. In FSW, this transformation is a complex process which involves friction, wear, adhesion, deformation, and recrystallization of material. [23]. For semi-crystalline materials such as PPS and PEEK, the FSW process works in the mix of material's crystal phases and glass phases. One of the aims of this process is to generate thermal energy by friction to heat up the material within the operating temperature range. This range starts from the glass transition temperature (T_g), and ends below the melting point (T_m) of the thermoplastics.

2.5 Mathematical Formulation

Heat generation phenomenon is found during the friction stir weld-creation process. Since FSW is a welding procedure that uses a welding tool to join the workpieces, the welding tool delivers activation energy to the workpieces and the joining of the workpieces is achieved while heat generates. In FSW, the mechanical power, P_m, is the amount of input source of energy transformed into heat per unit time. If η represents heat transformation efficiency, the total amount of heat, Q_t, generated in a particular time interval, T, during FSW can be expressed as,

$Q_t = \eta\, P_m\, T,\ 0 \leq \eta \leq 1$, when, P_m *is constant*

For simplification, if all of the mechanical power is transformed into heat (assuming $\eta = 1$), the total heat generated by pin and rotating shoulder becomes,

$Q_t = Q_{pin} + Q_{sh}$

As mechanical power is the product of angular velocity (ω) and torque on the welding tool (M), we can write:

$$Q_t = (\omega MT)_{total}$$

$$= (\omega\, r_o\, F_{tp}\, T)_{pin} + \left(\int_{ro}^{rs} r\omega\, F_{ts}\, T dr\right)_{shoulder}$$

$$= (\omega\, r_o\, \tau\, A\, T)_{pin} + \left(\int_{ro}^{r} \omega\, r\, \tau\, A\, T\, dr\right)_{shoulder} \ldots\ldots\ldots\ldots\ (1)$$

Where, F_{tp} = tangential force at the perimeter of the pin, F_{ts} = tangential force at the perimeter of the shoulder, r = radial distance of the perimeter force, r_o = pin radius, r_s = shoulder radius, τ = contact shear stress, A = contact surface.

Since heat is generated at or near the active contact surfaces due to the rotational movement, the total amount of heat is the addition of the heat generated at all the contact surfaces. Thus,

$Q_t = Q_{pin} + Q_{ss}$

$Q_t = Q_{pt} + Q_{po} + Q_{ss}$ ……..*(2)*

Where, Q_{pt} = the amount of heat produced at pin tip, Q_{po} = the amount of heat produced at pin outer surface, Q_{ss} = the amount of heat produced at shoulder bottom surface.

In addition to frictional heat, deformational heat is also produced during the welding phase. Deformational heat is produced by one of the basic tribological processes known as pure sticking [23]. Pure sticking assumes shearing in the layer of the material of the weld pieces very close to the contact surface and uniformity of the shear stress, τ. In this situation, the surface of the weld piece will stick to the rotating tool's surface only if friction shear stress exceeds the yield shear stress of the weld piece [23]. Thus, the total heat generated during FSW is a function of pure friction, pure deformation and a combination of friction and deformation. If we define δ as a dimensionless contact state variable such that

δ = 0 for pure frictional heat

δ = 1 for pure deformational heat

0< δ < 1 for combination of frictional and deformational heat

Then, heat components generated by the different active contact surfaces are:

$Q_{pt} = (1- \delta)\, Q_{pt,\, friction} + \delta\, Q_{pt,\, deformation}$

$Q_{po} = (1- \delta)\, Q_{po,\, friction} + \delta\, Q_{po,\, deformation}$

$Q_{ss} = (1- \delta)\, Q_{ss,\, friction} + \delta\, Q_{ss,\, deformation}$

Considering frictional and deformational heat production, contact shear stress in equation (1) can be expressed as:

$$\tau = \begin{cases} \mu p, & heat\ generation\ due\ to\ friction \\ \tau_{yield}, & heat\ generation\ due\ to\ deformation \end{cases}$$

Where, μ = friction coefficient, p= contact pressure, τ_{yield} = shear yield strength

To quantify the total heat generation analytically during friction stir welding of PPS and PEEK analytically, the friction coefficient between weld piece and welding tool [32], contact pressure of the tool to the weld piece and the shear yield strength of the material have to be determined. The Von Mises yield criterion in uniaxial tension and pure shear condition can be used to approximate the boundary value of tangential shear yield stress. The shear yield strength of the polymer is a function of temperature and strain rate. This requires the full temperature and strain history of the workpieces in a wide zone around the welding tool [23] [33]. By looking into the active contact surfaces in the different welding phases and the analytical model of heat generation, it is evident that the maximum heat is generated during the welding phase. Unlike metals, thermoplastic polymers have low coefficients of friction (for PPS: 0.2, for PEEK: 0.11 and for aluminium 1.05-1.35) and low thermal conductivity (for PPS: 0.19 W/m-K, for PEEK: 0.240 W/m-K and for aluminium 2024: 121-193 W/m-K). For these reasons, only a limited amount of heat is generated as a result of friction and deformation, and the propagation of this heat is very slow through the weld pieces.

2.6 Addition of External Heat Sources

To enable joining of thermoplastic using FSW, preheating of the weld pieces is introduced in this study. External heat can be added to the weld pieces from bottom and/or top surfaces (Figure 2.4). This additional external heating is applied to elevate the temperature of the weld pieces required for the welding process. This heat is added in

addition to the heat generated by the frictional and deformational heating process. To have a good control over the heating process, let us consider this external heating system as a primary heat source, Q_p, while frictional and deformational heat are the secondary heat source, Q_s. Therefore, Total amount of heat, Q_T will be the addition of both heat sources. Thus,

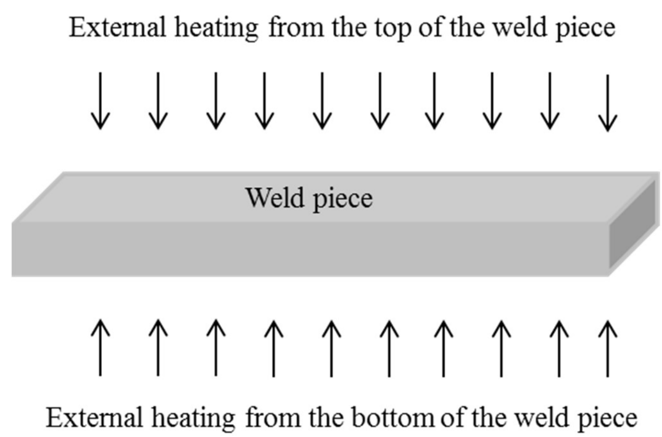

Figure 2.4: Concept of external heating from bottom and top of the weld piece

$$Q_T = Q_p + Q_s \quad \ldots\ldots\ldots\ldots\ldots\ldots\ldots\ldots\ldots\ldots\ldots\ldots\ldots\ldots\ldots\ldots\ldots\ldots\ldots (3)$$

Where, $Q_s = Q_{pt} + Q_{po} + Q_{ss}$

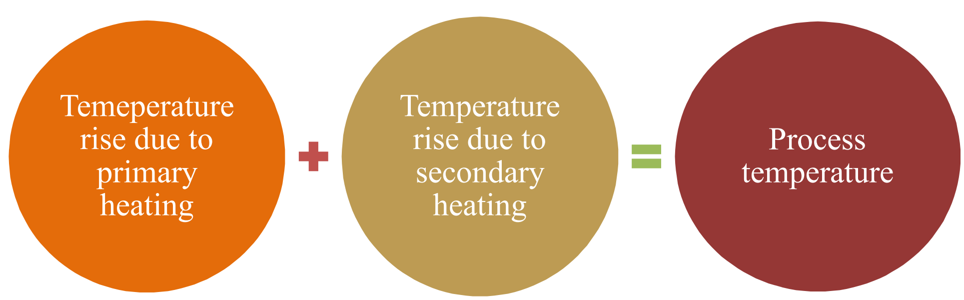

Figure 2.5: Process temperature is the combination of primary and secondary heating

The role of the primary heat source is to preheat the weld pieces before the plunge phase starts. This preheating keeps the weld pieces heated below the process temperature. The secondary heat, generated by the friction and deformation caused by the FSW tool and the weld pieces, is used to reach the temperature required for the welding environment. Combination of primary and secondary heating softens the materials and makes it susceptible to stirring and mechanical joining.

The external heat can be transferred to the weld piece using a conduction and/or radiation process. If we use a radiation process, the heat source will be placed at some distance from the weld piece. Example of such heat source can be infra-red heater (IR heater). Since the welding is performed on the top surface of the weld piece, radiation process of heat transfer can be applied to the weld piece. On the other hand, if we use conduction process, the heater needs to be placed at the bottom and in contact of the weld piece. If the external heat sources remain in contact with the weld pieces, diffusion of heat from the external heaters occurs due to the temperature difference between the heater and the weld piece. The heat diffusion equation is described as:

$$k\left(\frac{d^2T}{dx^2}+\frac{d^2T}{dy^2}+\frac{d^2T}{dz^2}\right)+q=\frac{1}{\alpha}\frac{dT}{dt} \quad \text{.....(4)}$$

Where T=Temperature, q=heat flux, k=conductivity, (x,y,z) = spatial coordinates, t=time, α = positive constant.

While designing the experimental setup of this study, resistance type surface heaters are utilized as the primary heat source, which were in contact with the weld piece. As suggested by the equation (4), heat is diffused in x, y and z direction. However, the heat propagating in z-direction only is the effective heat energy to heat up the weld pieces.

When externally controlled heat is used either from the top or bottom of the weld pieces, there remains a temperature gradient along the thickness of these pieces due to the low thermal conductivity of the polymer. In this study, a relatively large thickness of the weld pieces was used and, therefore a relatively large temperature gradient was observed.

2.7 Chapter Summary

In this chapter, different phases of the friction stir welding process have been described. In total five phases have been identified where the initial dwelling phase, welding phase and final dwelling phase were generating heat. During each of the phases, active contact surfaces have been determined that contribute to the heat generation process. A mathematical formulation has been developed to estimate the heat generation during the welding process. In case of welding of thermoplastic material, it is observed that the heat generated during the FSW process is not sufficient to soften the weld piece which is required for their joining. Therefore, an external heat source needs to be added to the welding equipment which is different from the FSW of metals. This external heat source, which can be applied from the top and/or bottom of the weld pieces, acts as a primary heat source for preheating of the weld pieces. External heating with resistance type surface heater was considered during the experimental setup design of this study.

CHAPTER 3

EXPERIMENTAL SETUPS FOR FRICTION STIR WELDING

The design of the experimental setup was based on the functions to be performed by the friction stir welding system. During the design the friction stir welding system, cost, flexibility, quality of process and ease of use were emphasized. The expected functionalities to be performed by this system and probable means to achieve these functionalities were as follows:

- Properly holding the samples in place during all the phases of FSW: Clamping system
- A way of generating friction as well as stirring of materials: Tool with rotation
- Applying z-directional force to keep the stirred materials into the weld line: Shoulder arrangement
- A way to move the friction and stirring process along the weld line: Tool transverse motion.

A conventional 3-axis milling machine with clamping mechanism was used in this research. While performing initial experiments with this setup it was found that the heat produced by the friction and deformation was not able to join thermoplastic materials. This led to the introduction of external heating system to the experimental setup. Based on the type of shoulder arrangement, two types of experimental setups were used. Figure 3.1 shows a 3D representation of experimental setup 1, which consists of

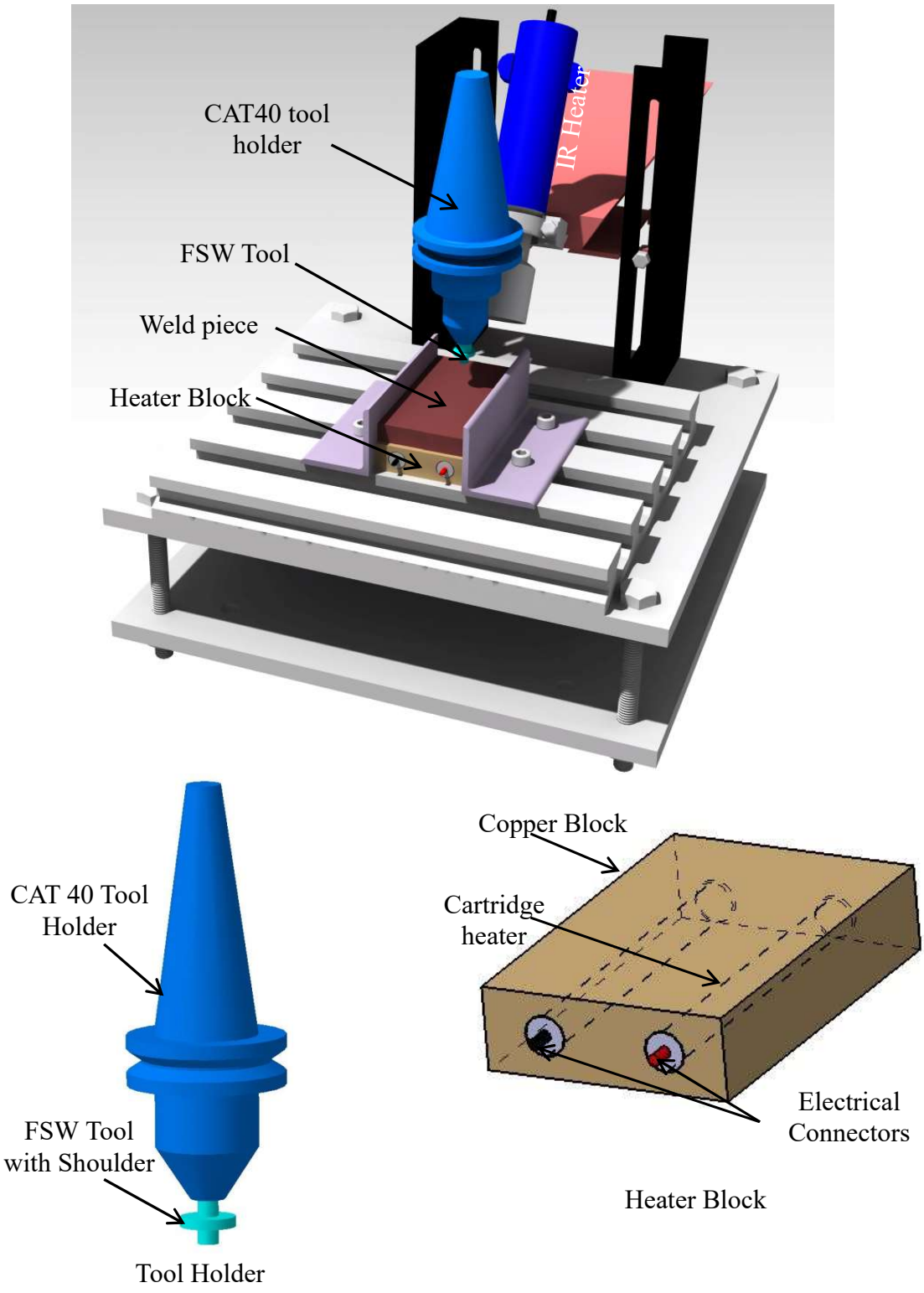

Figure 3.1: Setup 1- a 3D representation of experimental setup consisting of top and bottom heater along with rotating shoulder

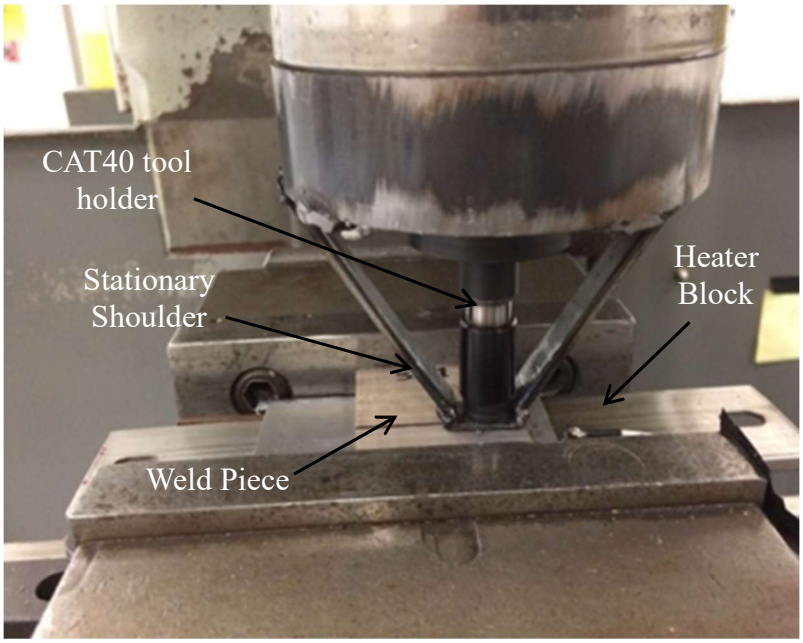

Figure 3.2: Setup 2- experimental setup consisting of bottom heater along with stationary shoulder.

two types of external heating system along with rotating shoulder: heating from top of the sample and from bottom of the sample. In this study, only a bottom heater was utilized.

Figure 3.2 shows the second type of experimental setup, which consists of bottom heater along with stationary shoulder. A conventional 3-axis milling machine was used for both of these experimental setups for tool rotation and transverse motion. Vertical height of the tool is adjusted according to the depth required by the tool pin. Major parts of this experimental setup are as follows:

Milling Machine (quantity 01): A Dynapath Delta CNC (Model: Delta – 40MU) controlled Journeyman 425 3-axis milling machine is used for FSW process. To run the machine in automatic mode, G-codes were developed. A sample of these G-Codes is attached in Appendix A.

Figure 3.3: Journeyman 425 Milling machine with Dynapath CNC control

Tool holder (quantity 01): A standard holder (CAT40) is used to hold the FSW tool.

Surface heater (quantity 01): Two types of heater are used. For initial experiments, cartridge heaters inserted into a copper block is used as a primary heater. While performing experiments with cartridge heaters, it was found that the temperature along the weld line was varying at different locations. For this reason, a channel strip heater (203 mm x 38 mm x 7.5 mm) is used as the second type of primary heater. Total power of the strip heater is 250W and watt density is 13 watt/in^2. The maximum temperature that can be achieved by the strip heater is 650°C.

Clamp (quantity 02): Two clamps made of 2-in angle bar are used to hold the weld piece along with the heater block. These clamps keep the fixture in place during the welding process.

Tool: In these experimental setups, threaded bolts (*Zinc coated Mild Steel bolts*) are used as the tool pin. The bolts have a diameter of 5 mm and contain 20 threads per inch throughout their nominal length. Zinc plated flat washers with an inner diameter slightly

larger than the bolt's outer diameter are utilized as the rotating shoulder in the experimental setup 1. The washers had an inner diameter of 6 mm and outer diameter of 14 mm with a thickness of 1.2 mm. This shoulder arrangement is free to rotate with the rotational movement of the bolt. The bolt is inserted into the tool holder up to its shoulder as described in Figure 3.4. The rotational speed of the shoulder (i.e. washers) during the welding phase is not the same as the rotational speed of the bolt due to the friction between the workpiece and the washers.

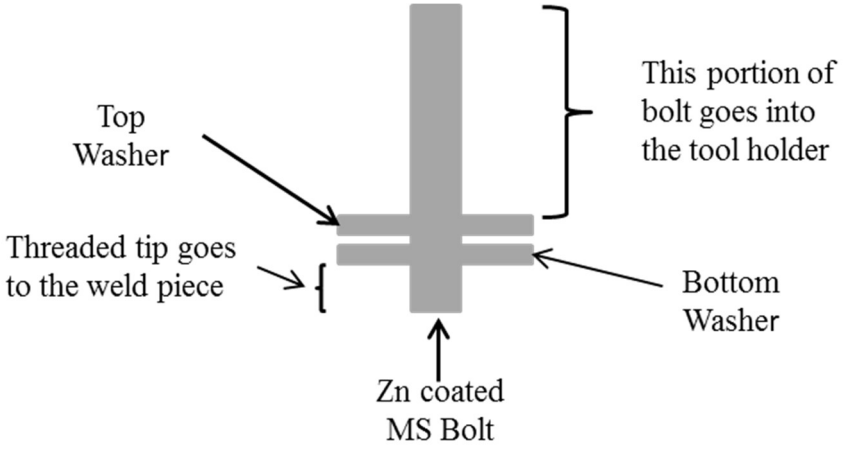

Figure 3.4: Drawing of tool with 2 washers as shoulder

Figure 3.5: FSW tool with one washer as a shoulder

Stationary shoulder: A stationary shoulder does not rotate with the tool in contrast to a rotating shoulder. Figure 3.2 shows the stationary shoulder arrangement used in the experiments.

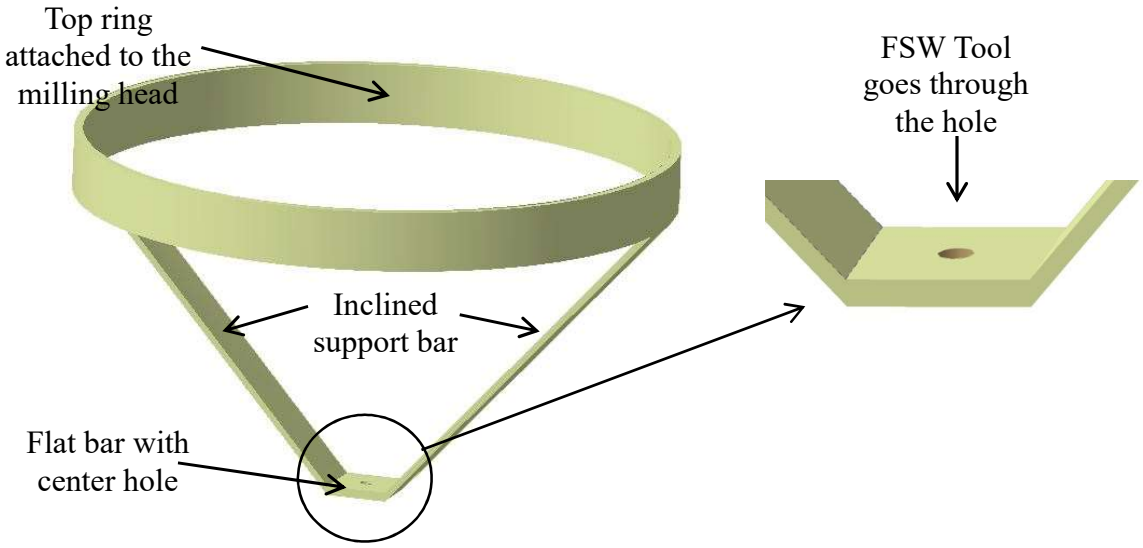

Figure 3.6: Stationary shoulder arrangement

Temperature control system: A closed loop feedback control system was developed to control the preheating temperature of the weld piece. This system was designed to get a fixed temperature at the bottom of the weld piece.

Following electrical components were used to develop this control system:

a) Temperature Controller: INKBIRD temperature controller.

b) Solid state relay: FOTEK SSR-25DA

c) Thermocouple: Copper-Constantan type T thermocouple

d) Voltage regulator: AUBER solid state voltage regulator (SSVR 25A)

The overall circuit diagram was as follows:

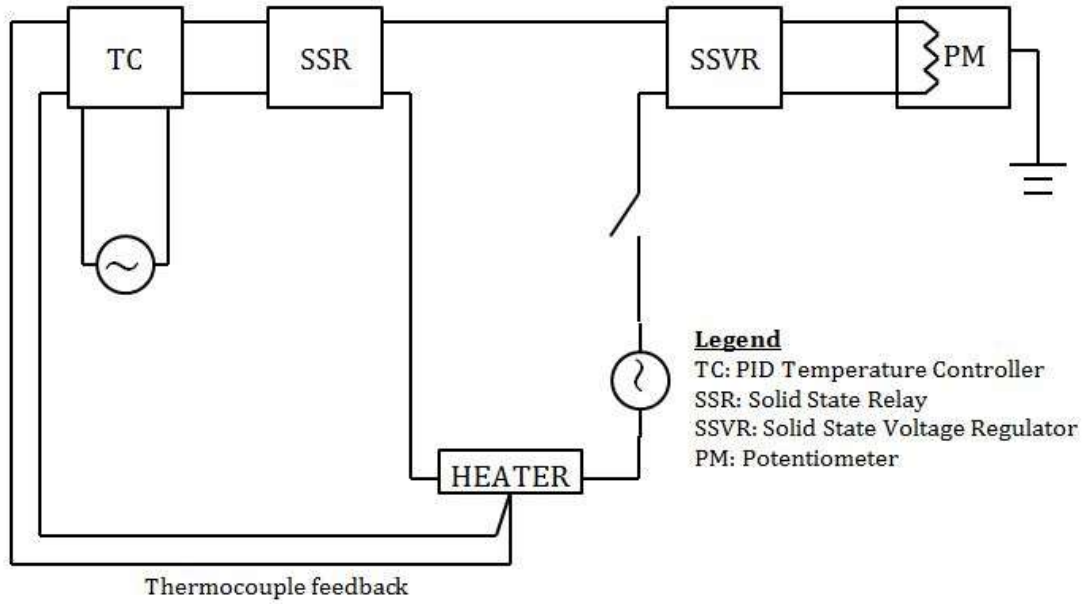

Figure 3.7: Closed loop feedback control system

The specimens were placed on the surface heater and the thermocouple was placed at the bottom of the specimens (Figure 3.8). The temperature indicated by the thermocouple was the bottom surface temperature of the weld piece.

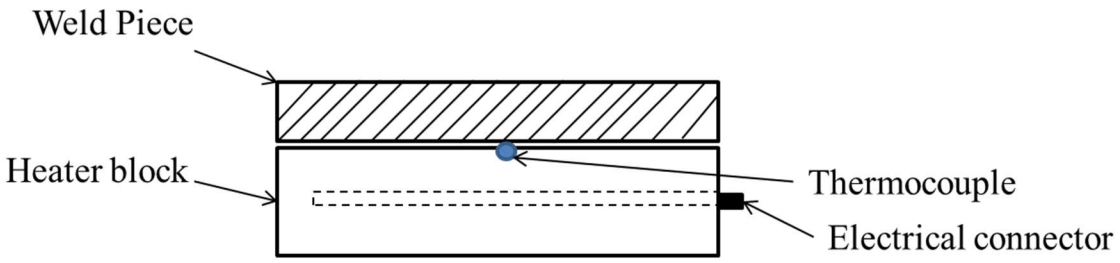

Figure 3.8: Positioning of the thermocouples

CHAPTER 4

DEVELOPMENT OF FRICTION STIR WELDING PROCESS FOR UNREINFORCED PPS

4.1 Background

Polyphenylene sulfide is an advanced engineering plastic, commonly used today as a high-performance thermoplastic. It is a semicrystalline polymer that has excellent dimensional stability under most environmental conditions. Its chemical structure is composed of alternating sulfur atoms and phenylene rings in a para substitution pattern (Figure 4.1). It possesses self-extinguishing properties without the addition of any flame retardant chemical additives which makes it suitable for aerospace application. The PPS used in this study was supplied by Quantum Polymer Corporation. This material was unreinforced (natural and unfilled) and extruded from prime virgin resin.

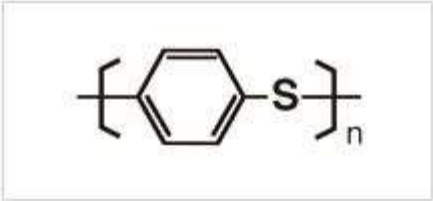

Figure 4.1: Chemical structure of PPS

Some of the researchers used friction stir spot welding technique to join thermoplastic polymers [34]. M K Bilici [15] performed an experimental and numerical analysis of friction stir spot welding of high density polypropylene. In this analysis, Taguchi approach was used as a statistical design of experiment technique to set the

optimal welding parameters. Use of this approach helped improve about 47.7% of weld strength from the initial welding parameters to the optimal welding parameters. Dwell time was the most dominant welding parameter and the tool rotational speed was the least important welding parameter in these experiments. In this study, the application of continuous friction stir welding method on PPS was developed by identifying the proper mix of process parameters.

4.2 Determination of Thermal Properties of PPS

The glass transition temperature (T_g) and the melting point (T_m) of this commercial PPS were determined. These values were determined using Differential Scanning Calorimetry. The samples were collected from the PPS plate and their weights were measured. The start temperature in DSC analysis was 30 °C and the samples were heated up to 400 °C with a heat rate of 20 °C /min. The samples were then cooled down to 30 °C with a heat rate of 50 °C /min. The lowest T_g of PPS was found as 116.93 °C and the average temperature of three samples was 118.96 °C. On the other hand, the melting point of the PPS sample was determined as 280 °C. The results obtained from DSC are presented in Figure 4.2.

4.3 Experimental Procedure

4.3.1 Sample dimension, type and preparation

In this study, two types of PPS samples were prepared. To determine initial process parameters, single piece test specimens were prepared from commercial PPS plates using a Benchtop Band Saw. The dimensions of these specimens was 75 mm x 50

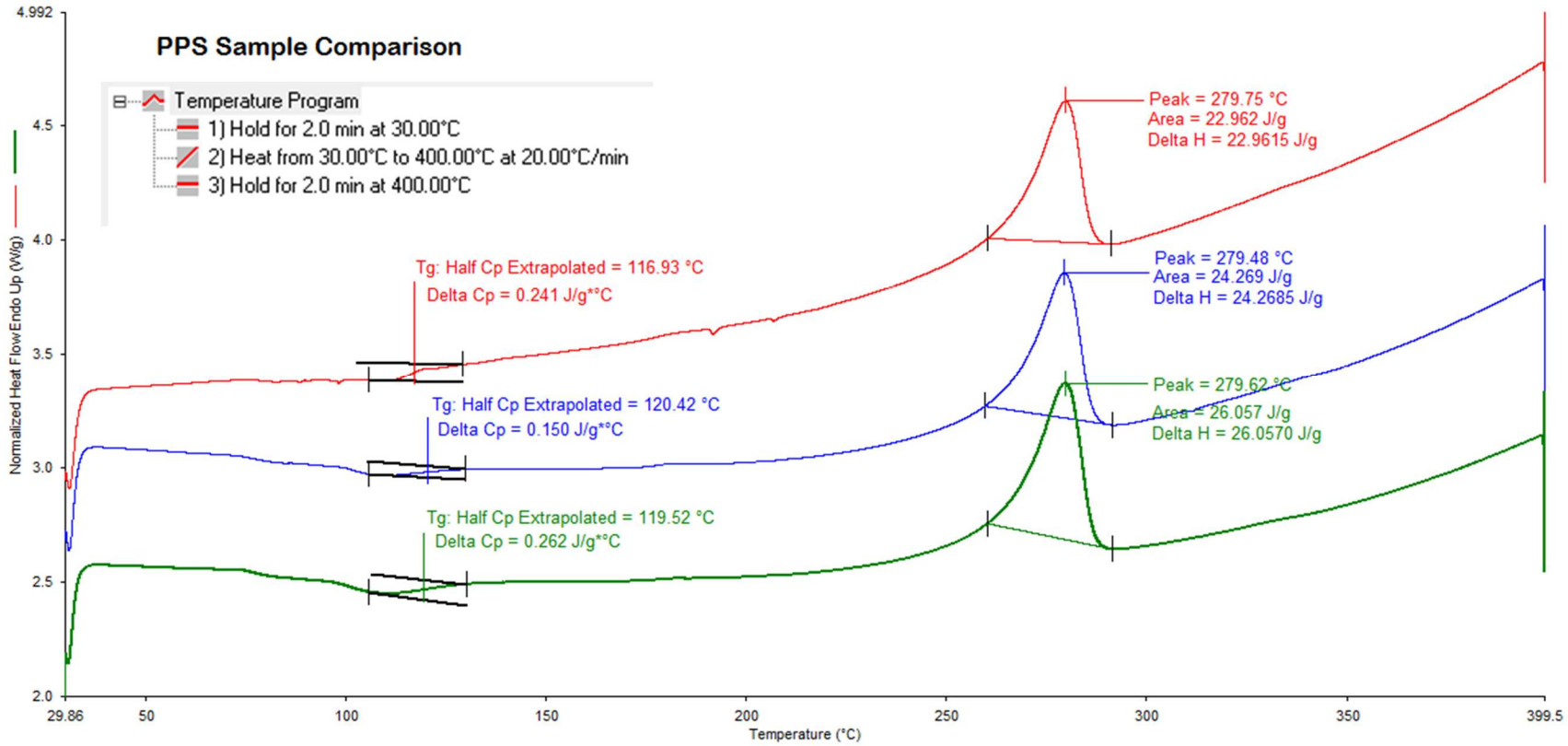

Figure 4.2: Determination of glass transition temperature and melting point of PPS using DSC.

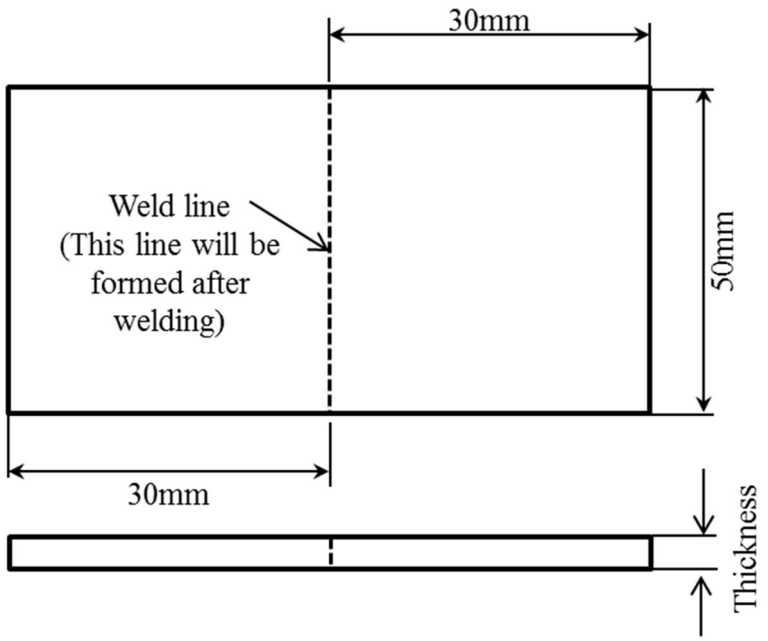

Figure 4.3: Two piece butt joint test specimen

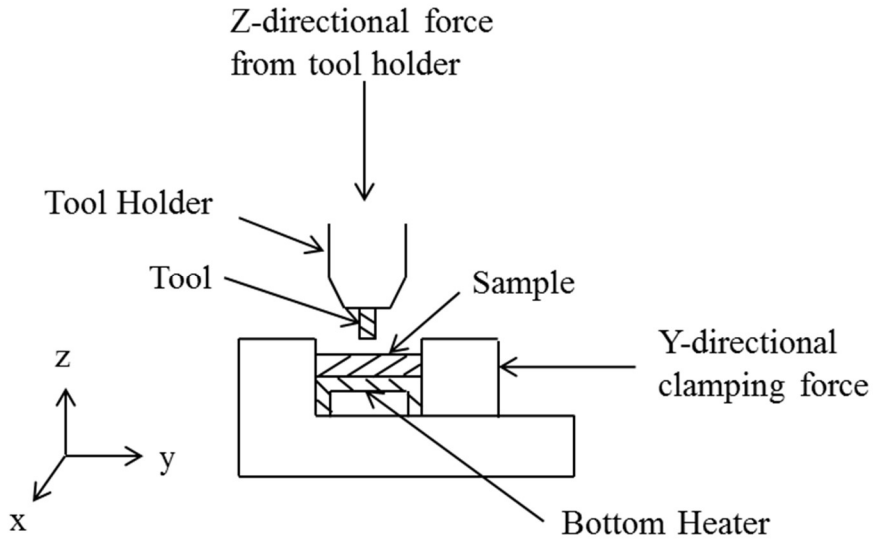

Figure 4.4: Clamping mechanism to hold the sample with a bottom heater

mm x 11 mm (L x W x T). To identify proper initial process parameters, two piece butt joint test specimen were prepared using Benchtop Band Saw and 3-axis milling machine. The thickness of the second type of specimen was 4±1 mm. The length and width of each sample were 50 mm and 30 mm (Figure 4.3).

To work with the milling machine the test specimen must be rigidly fixed on the milling table. A table vice was used to hold the specimen in place with a y-directional clamping force to accommodate the bottom heater (Figure 4.4). To remove any waviness or uneven surface, disc sanding machine was utilized. Figure 4.3 shows a two piece butt-joint specimen used to investigate the weld strength of friction stir welds under tensile loading conditions.

4.3.2 Experiment design

Development of friction stir welding method for unreinforced PPS was aiming to answer two questions: a) is it possible to weld unreinforced PPS and b) if yes, what are the process parameters that give the maximum quality characteristics. Therefore, the experiments were performed in two phases. In phase I, weldability of the PPS samples were determined. To do this, single piece test specimen were used, and the FSW process was continued until a reliable joint was found. Phase II was employed to identify the proper mix of the welding parameters to achieve the maximum tensile strength of the joint and uniform distribution of stirred material along the joint line.

4.3.3 Outcome of phase I and design of phase II

14 different tests were performed with rotating shoulder arrangement in phase I. During these tests, process parameters such as tool rotational speed, tool traverse speed and material bottom temperature were varied. The bottom surface temperature of the material was varied from 45°C to 175°C and the tool rotational speed was varied from 200 rpm to 900 rpm. 4 additional tests were carried out at higher tool rotational speed

(from 1000 rpm to 1400 rpm) without applying external heat. However, there was no sign of any welded joint rather PPS chips were observed and the run off was created.

In phase I, at some configuration of process parameters, promising weld line was found. The combination of the process parameters that gives continuous weld line was noted and taken as input parameters for phase II. Based on the results of phase I, welding parameters of phase II was designed. Four input variables or welding parameters that seemed to be influential on the weldability of PPS samples were identified from initial experiments. These were a) Heating duration, b) Material temperature before welding, c) Tool rotational speed, and d) Tool traverse speed.

In phase II, Taguchi's design of experiment was used to determine the relationship between the input variables and the output characteristics [35]. A Taguchi design is a designed experiment that lets its user to choose a product or process that functions more consistently in the operating environment [36]. Taguchi designs recognize that not all factors that cause variability can be controlled. These uncontrollable factors are called noise factors. Taguchi designs try to identify controllable factors (control factors) that minimize the effect of the noise factors. Taguchi designs are just highly fractionated factorial designs, and can distinguish between process variables and noise variables. This method enables its user to design orthogonal array and perform analysis of variance (ANOVA).

To implement Taguchi's method, different levels of each of the process variables were proposed to identify the proper mix of process variables to achieve maximum tensile strength of the PPS joint. These variables were selected based on the weldability found in phase I. Proposed values of each of the variables are described below:

Material temperature: In phase I, good weld was found when the process temperature (due to the combination of primary and secondary heat) was little above the glass transition temperature but well below the melting point of the PPS sample. For example, good weld was not observed below 65°C or beyond 100°C of preheat temperature. Moreover, at 85°C, promising weld was found with varying rotational speed of the tool. Therefore, three different temperatures were taken into account for preheating of the samples. These were 65°C, 85°C and 100°C.

Heating duration: If a semi crystalline polymer is heated above its glass transition temperature, the amorphous region will become mobile and this mobility will impact its mechanical properties [37]. It was anticipated that the heating duration will promote the mobility of the amorphous region, and thus it can be considered as a process variable. To reduce the number of trials, only two levels of heating duration were considered to investigate whether it had any influence on the tensile strength of the welded samples. They were 10 minutes and 20 minutes. When the material temperature reached a preselected value (65°C or 85°C or 100°C), the duration of heating counted from this point (Figure 4.5).

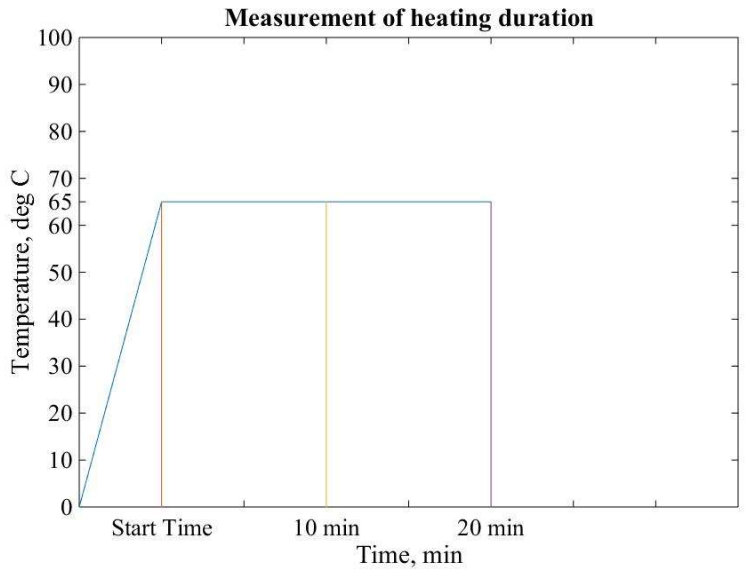

Figure 4.5: Concept of measuring heating duration

Tool rotational speed: Tool rotational speed is the source of frictional heat produced during welding phase of FSW process. It was observed in phase I that a speed lower than 600 rpm and a speed higher than 900 rpm did not yield promising weld. Three evenly distributed levels of tool rotational speed were considered for Taguchi design: 675 rpm, 775 rpm and 875 rpm.

Tool traverse speed: This parameter is one of the determining factors whether the process is a milling operation or a joining operation. When combining with the other parameters (material temperature and tool rotational speed), three levels of tool traverse speed was considered based on the observations in phase I. They were 2 mm/min, 5 mm/min and 8 mm/min.

All the values of these 4 variables were arranged in an orthogonal array using statistical software named ‘Minitab’. Using Minitab, one can determine the number of minimum trials required to optimize the output variable utilizing its ‘Design of Experiment’ tab. This software determines the number of trials on the basis of input

levels of each of the input variables and uses fractional factorial design method. In a full factorial design a total of 54 (2 x 3 x 3 x 3) trials are required where 2-factor and 3-factor interactions between the input variables are considered.

Table 4.1: Process variables and their levels, L_{18}- a $2x3^3$ fractional factorial design

Trial no	*Heating Duration (min)*	*Material Temperature (°C)*	*Rotational Speed (RPM)*	*Traverse Speed (mm/min)*
1	*10*	*65*	*675*	*2*
2	*10*	*65*	*775*	*5*
3	*10*	*65*	*875*	*8*
4	*10*	*80*	*675*	*2*
5	*10*	*80*	*775*	*5*
6	*10*	*80*	*875*	*8*
7	*10*	*100*	*675*	*5*
8	*10*	*100*	*775*	*8*
9	*10*	*100*	*875*	*2*
10	*20*	*65*	*675*	*8*
11	*20*	*65*	*775*	*2*
12	*20*	*65*	*875*	*5*
13	*20*	*80*	*675*	*5*
14	*20*	*80*	*775*	*8*
15	*20*	*80*	*875*	*2*
16	*20*	*100*	*675*	*8*
17	*20*	*100*	*775*	*2*
18	*20*	*100*	*875*	*5*

In this study, mixed level variables (one 2-level variable and three 3-level variables) are used and all interactions (for example: Material Temperature x Rotational Speed x Traverse speed) are assumed to be zero. Thus from the orthogonal array, it was found that 18 ($2 \times 3^{3-1}$) trials had to be performed, which are presented in Table 4.1. The

butt-joint tensile strength was obtained by averaging the strengths of three individual specimens, which were welded with identical welding parameters.

Legends used for describing process variables

To indicate the values of process variables following legends will be used in this study:

HDx : Heating Duration and 'x' will be the value in minutes

MTx : Material temperature and 'x' will be the value in degree Centigrade

RSx : Rotational Speed of the tool and 'x' will be the value in RPM

TSx : Traverse Speed of the tool and 'x' will be the value in mm/min

Example: HD10MT65RS675TS2 means

Heating Duration : 10 minutes

Material temperature : 65°C

Rotational Speed : 675 RPM

Traverse Speed : 2 mm/min

4.3.4 Minimization of noise factors

In Taguchi designs, factors that cause variability in the performance of a process or product, but cannot be controlled during the production process are known as noise factors. These unavoidable noise factors can be controlled or simulated during experimentation. These noise factor levels should be chosen in a way that represents the range of conditions under which the outcome or response should remain robust. Types of noise factors that are considered in this study are as follows:

External environmental factors

Temperature, humidity and wind velocity: All these factors can be considered constant in a controlled laboratory environment as such the variation of heat flow rate to the specimen was negligible.

Manufacturing variations

Part to part variation: Entire specimens were prepared from the commercial PPS plates as received condition. The internal variations in the density and void contents of each plate were out of control. However, it can be considered that these factors were fairly constant throughout the plates as theses plates were manufactured by extrusion process.

Measurement variations

The variations in measurement method and tools cannot be controlled. However, the tool rotational speed and tools traverse speed were measured with a calibrated 3-axis CNC machine and thus the measurement variations can be considered minimum. The material temperature and heating duration were measured with the identical thermocouple and digital watch.

4.4 Results and Discussion

4.4.1 Surface morphology of welded samples

In all trials, at least three welded samples were produced. The surface morphology of the welded samples varied from rough finish to smooth finish. Images of some of the welded samples are appended in Figure 4.6, Figure 4.7 and Figure 4.8. It can be noted in Figure 4.7 that the process variables are same whereas the surface morphology is

different. This can be due to the variations in z-directional force during the welding phase.

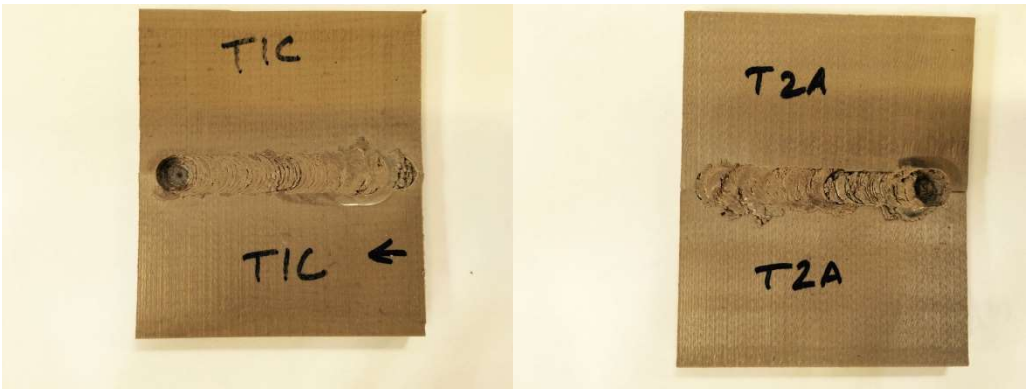

Figure 4.6: (left) HD10MT65RS675TS2, (right) HD10MT65RS775TS5

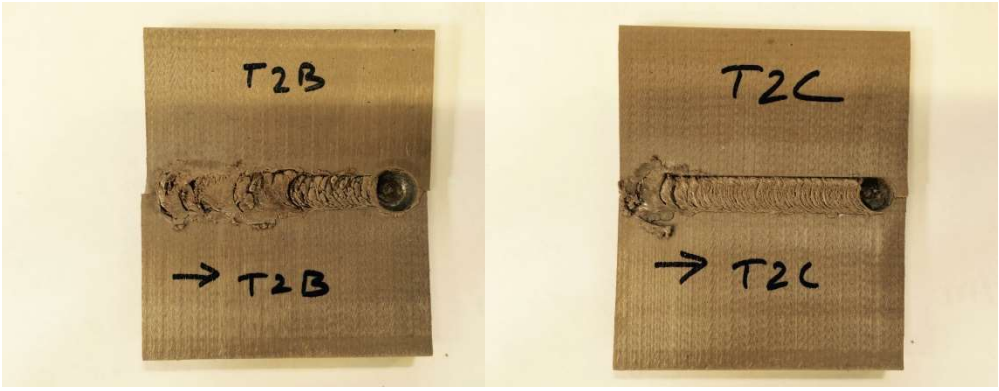

Figure 4.7: (left) HD10MT65RS775TS5, (right) HD10MT65RS775TS5

Figure 4.8: (left) HD10MT80RS775TS5, (right) HD10MT80RS775TS5

It was also observed that there was a temperature difference between the bottom surface and the top surface of each sample. Due to this difference in temperature, bottom surface of each sample was expanded more than the top surface. This uneven material expansion and sidewise clamping force resulted in some degree of bending of some of the samples. The bend in one PPS sample is shown in Figure 4.9.

Figure 4.9: Welded PPS sample with uneven expansion.

4.4.2 Determining tensile strength

As mentioned earlier, the response variable or the output characteristics of the welded sample was the tensile strength. To determine the tensile strength, ASTM D638 standard was used as the basis for the tensile tests. These strengths were measured using a MTS machine where the speed of test was 5 mm/min. The tensile strengths of the welded PPS samples are shown in Table 4.2.

4.4.3 Signal to noise ratio

The Taguchi method uses the signal to noise (S/N) ratio [35]. The last column of Table 4.2 shows the calculated S/N ratio of the experiments. The term ‘signal’ represents the desirable value (mean) for the output characteristic, and the term ‘noise’ represents the undesirable value for the output characteristic. Therefore, the S/N ratio is the ratio of

the mean to the square deviation. Taguchi uses the S/N ratio to measure the quality characteristics deviating from the desired value. The S/N ratio, Ƞ is defined as [38]:

$$\text{Ƞ} = -10\log(\frac{1}{n}\sum_{i=1}^{n}\frac{1}{T_i^2}) \quad \ldots\ldots \ldots\ldots (2)$$

Table 4.2: Experimental results for weld strength with different welding parameters and calculated S/N ratios.

Trial No	*Heating Duration (min)*	*Material Temp. (°C)*	*Rotational Speed (rpm)*	*Traverse Speed (mm/min)*	*Tensile Strength (MPa)*	*Mean Square Deviation*	*Signal to Noise Ratio*
1	*10*	*65*	*675*	*2*	*9.85*	*0.01*	*19.87*
2	*10*	*65*	*775*	*5*	*2.87*	*0.12*	*9.17*
3	*10*	*65*	*875*	*8*	*1.10*	*0.83*	*0.81*
4	*10*	*80*	*675*	*2*	*9.51*	*0.01*	*19.56*
5	*10*	*80*	*775*	*5*	*6.21*	*0.03*	*15.86*
6	*10*	*80*	*875*	*8*	*9.41*	*0.01*	*19.47*
7	*10*	*100*	*675*	*5*	*6.63*	*0.02*	*16.42*
8	*10*	*100*	*775*	*8*	*3.94*	*0.06*	*11.91*
9	*10*	*100*	*875*	*2*	*10.17*	*0.01*	*21.45*
10	*20*	*65*	*675*	*8*	*2.23*	*0.20*	*6.97*
11	*20*	*65*	*775*	*2*	*9.65*	*0.01*	*19.69*
12	*20*	*65*	*875*	*5*	*9.15*	*0.01*	*19.23*
13	*20*	*80*	*675*	*5*	*4.88*	*0.04*	*13.76*
14	*20*	*80*	*775*	*8*	*3.86*	*0.07*	*11.74*
15	*20*	*80*	*875*	*2*	*4.25*	*0.06*	*12.57*
16	*20*	*100*	*675*	*8*	*3.76*	*0.07*	*11.50*
17	*20*	*100*	*775*	*2*	*7.31*	*0.02*	*17.28*
18	*20*	*100*	*875*	*5*	*2.54*	*0.16*	*8.10*

The term inside the logarithm parenthesis is the mean square deviation (MSD) for the output characteristics. In the study of structural strength, the higher-the better quality characteristics are considered [39]. In eq. (2), n is the number of tests and T_i is the value

of weld strength of the i^{th} test. In Table 4.2, the experimental results for the weld strength and the corresponding S/N ratios are shown. These S/N ratios were calculated by using Equation (2).

In these tests, 18 different welding parameter combinations were used. Therefore, the effect of each welding parameter on the weld strength cannot be clearly understood from the results shown in Table 4.2. The Statistical Package for the Social Sciences (SPSS) software was used to explain the welding parameter effect.

Table 4.3: S/N response table

Welding Parameters	*Mean S/N ratio (dB)*				*Mean*
	Level 1	*Level 2*	*Level 3*	*Max-min*	
Heating Duration	*14.80*	*13.43*	*--*	*1.38*	*14.12*
Material Temp	*12.62*	*15.49*	*14.23*	*2.87*	*14.12*
Rotational Speed	*14.68*	*14.28*	*13.39*	*1.30*	*14.12*
Traverse Speed	*18.19*	*13.76*	*10.40*	*7.79*	*14.12*

Since the experimental design is orthogonal, it is then possible to identify the effect of each welding parameter on S/N ratio at different levels. For example, the mean S/N ratio for material temperature at levels 1, 2 and 3 can be determined by averaging S/N ratios for the experiments set 1 (Trial no 1, 2, 3, 10, 11, 12), set 2 (Trial no 4, 5, 6, 13, 14, 15), and set 3 (Trial no 7, 8, 9, 16, 17, 18) respectively. These results are shown in Table 4.3. This table also shows the mean S/N ratio for each level of the welding parameters. It can be noted from Table 4.3 that the largest change of S/N ratio (Max-min)

was occurred by traverse speed, which was 7.79 dB. The total mean S/N ratio of the 18 experiments was calculated as 14.12 dB.

The S/N response graph for the weld strength was drawn using the results shown in Table 4.3. The graphs in Figure 4.10 show the level effects of each welding parameter. In Figure 4.10, the dashed line shows the total mean S/N ratio (14.12 dB) of the experiments. For example, the mean S/N ratio decreases as the heating duration levels increases from 10 minutes to 20 minutes. That means that the weld strength decreases with an increase of the heating duration. Similar effect was found for the case of traverse speed. That is, if the traverse speed is increased, the weld strength is decreased. However, the degree of effect of traverse speed on the weld strength is larger than that of heating duration on the weld strength.

4.4.4 Analysis of variance

The relative effect of the different welding parameters on the tensile strength was acquired by the disintegration of variance, which is known as analysis of variance (ANOVA). The purpose of ANOVA is to understand which variable(s) highly affect the output quality feature statistically. In this study, the ANOVA was performed by separating the total variability of the mean tensile strength of the welded joints into contributions by each of the welding parameters and error. The results of ANOVA for mean tensile strength is shown in Table 4.4, which was generated by SPSS.

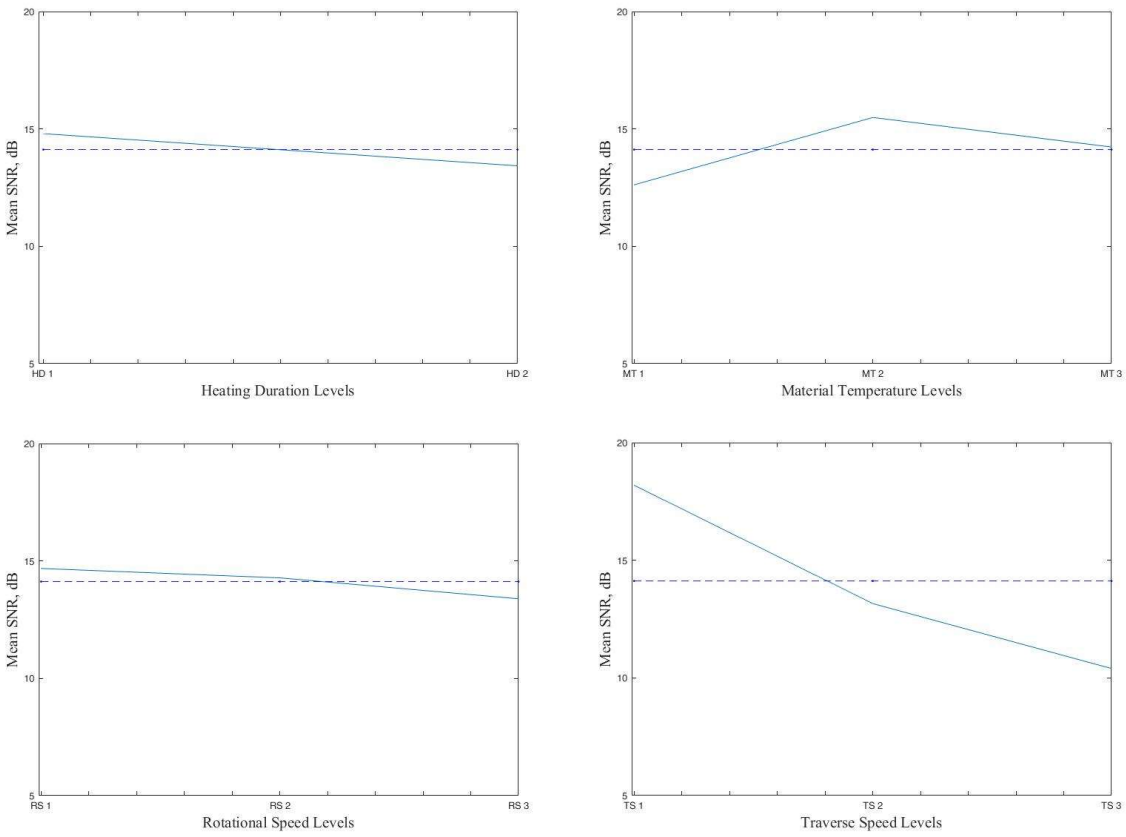

Figure 4.10: The mean S/N response graph for notched weld strength

Table 4.4: Test of Between-Subjects effects

Source	*Sum of Squares*	*DOF*	*Mean Square*	*F*
Corrected Model	*71.73[a]*	*7*	*71.73*	*1.009*
HD	*8.07*	*1*	*8.07*	*1.009*
TEMP	*1.39*	*2*	*.697*	*0.087*
RS	*0.93*	*2*	*.466*	*0.058*
TS	*61.34*	*2*	*30.67*	*3.838*
Error	*87.90*	*11*	*7.99*	
Corrected Total	*159.64*	*18*		

The degree of freedom

In statistics, the number of independent ways by which a process or system can move or vary without violating any constraint imposed on it, is known as the number of degrees of freedom [40]. In statistical analysis of experimental results,

DOF of a factor = number of levels of the factor -1.

DOF of Heating Duration = 2 – 1 = 1.

Sum of squares

Total sum of the squared deviations (SS_T) between the welding parameters on the basis of the total mean tensile strength is calculated using following equation:

$$SS_T = \sum_{i=1}^{k} n_i(\bar{y}_{i.} - \bar{y}_{..})^2$$

Where, k = total number of level,

i =individual level,

n = number of experiment in each level

$\bar{y}_{i.}$ =value of mean response in each level

$\bar{y}_{..}$ = value of mean response in all levels

Example of calculation of SS_T for heating duration

Mean tensile strength corresponding to HD10 = 6.63 MPa

Mean tensile strength corresponding to HD20 = 5.29 MPa

Mean tensile strength of HD10 and HD20 = 5.96 MPa

SS_T for HD = 9 X $(5.96-6.63)^2$+9 X $(5.96-5.29)^2$

= 8.07

Mean of square deviations

The mean of squared deviations (SS_M) is equal to the sum of squared deviations (SS_T) divided by the number of degrees of freedom associated with the design parameter [15]. Thus the mean square deviation for the 'Heating Duration' is $\frac{SS_T}{DOF} = \frac{8.07}{1} = 8.07$.

F-Test

In statistics, there is a tool called an F test, which is named after the famous statistician R. A. Fisher, and is used to identify which design parameters have a significant effect on the quality characteristic. In performing the F test, the mean of squared deviations (SS_M) due to each design parameter are calculated. The F value for each of the design parameters is the ratio of the mean of squared deviations (SS_M) to the mean of the squared error.

F-value for heating duration:

Mean of square deviations = 8.07

Mean of the squared error = 7.99

F-value for heating duration = 8.07/7.99 = 1.009

In this study, the F-test was performed to study the importance of the welding parameters. If the F- ratio of any design parameter is higher than its critical value, then it can be concluded that the obtained F-ratio is likely to occur by chance with a significance level less than 5% [41]. That is the corresponding confidence level is 95%. In case of 'Traverse Speed' the value of F ratio is determined 3.838 which is higher than its critical value of 3.56 (Appendix B). In other words, with a 95% confidence level it can be concluded that the design parameter 'Traverse Speed' has significant influence on the output quality parameter.

4.4.5 Analysis of notched strengths of welded samples

While performing welding from the top of the specimen, tool penetration was not all the way to the bottom surface (Figure 4.11). This was because of the presence of surface heater at the bottom. Therefore, an un-welded portion was present in each of the samples (Figure 4.12). This un-welded part is similar to a crack or notch and will strongly influence the measured strength. Usually, the notch length varied depending on the tool penetration.

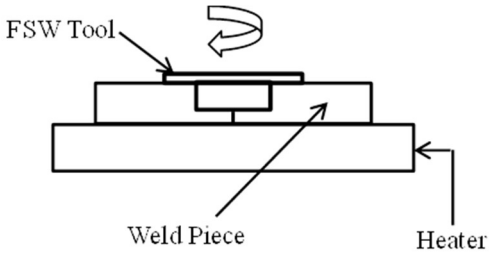

Figure 4.11 Weld pieces preheated by a bottom heater

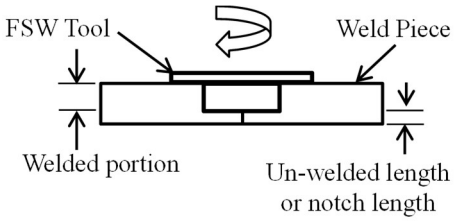

Figure 4.12: Un-welded portion close to the bottom of the weld piece

In this study, the tensile strengths of the welded samples were determined considering the notches or un-welded lengths. The un-welded portion acts as an edge crack or notch during the tensile test as shown in Figure 4.13. These strengths were then compared with the residual strength of the base material. The residual strength is the term used for the strength that remains in the part in the presence of a defect. To determine the

residual tensile strength, the fracture toughness needs to be determined for PPS. Fracture toughness is a material property and residual strength is the fracture stress of a structural part. The strength of a cracked part is a fraction of a similar un-cracked part. Therefore, 'residual' can be regarded as 'whatever is left' of a structure's load carrying capability. Considering plain stress condition, tensile strength and fracture toughness can be described as [42]:

$K_{IC} = c\ \sigma\sqrt{\pi a}$ …… ……..*(3)*

Where,

K_{IC} = Critical Fracture Toughness in mode I fracture

C = Geometry correction factor = 1.12 for semi-infinite plates [43]

σ = Residual Tensile Strength

a = Crack length

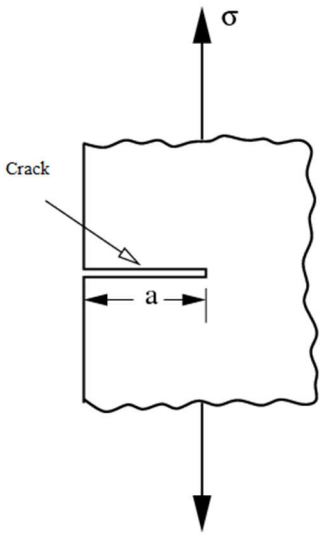

Figure 4.13 Influence of crack or un-welded section on residual strength.

To determine the fracture toughness of PPS, three identical compact test specimens were prepared where the speed of testing was 5 mm/min. The displacement

and corresponding tensile loads were recorded for each of the samples. The specified dimensions of the test specimen and the actual specimen are as follows:

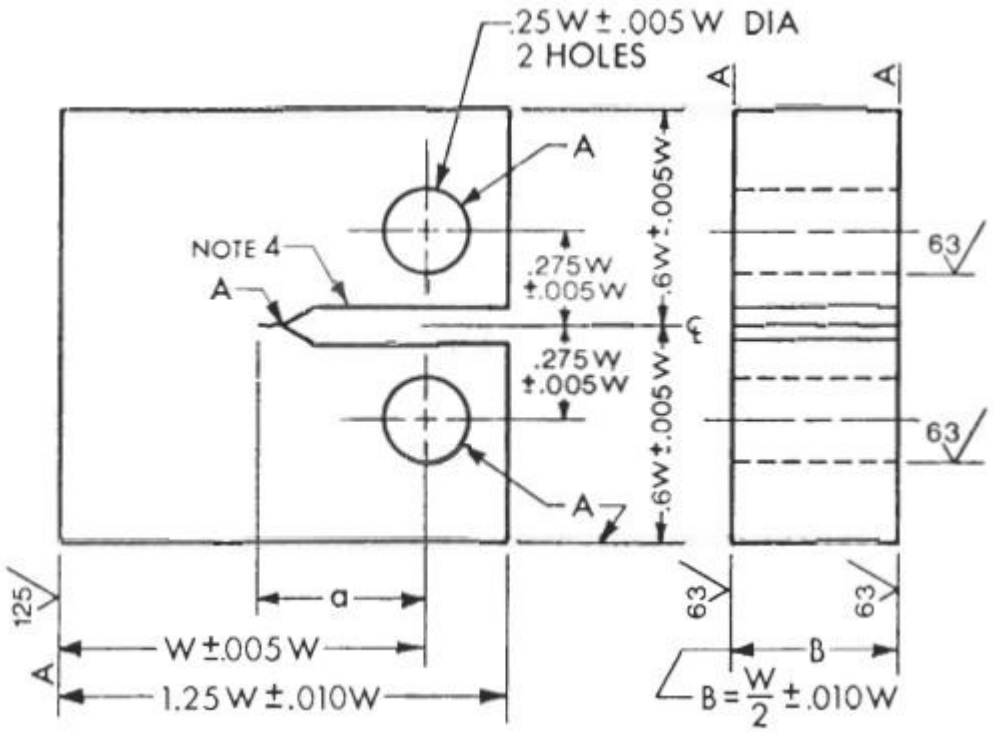

Figure 4.14: Compact test specimen standard proportions and tolerances

Figure 4.15: Actual PPS test specimen

Table 4.5: Specifications of PPS samples for K_{IC} testing

Value of B, mm	*Value of B, cm*	*Value of W, mm*	*Value of W, cm*	*Value of a, cm*	*a/w*	*f(a/W)*
11	*1.1*	*22*	*2.2*	*1.1*	*0.5*	*9.517657*

The stress intensity, K_Q was calculated using following equation:

$$K_Q = (P_Q/BW^{1/2}) * f(a/W)$$

Where,

$$f(a/W) = \frac{\left(2+\frac{a}{W}\right)*(0.866+4.6a*\frac{a}{w}-13.32*a^2/W^2+14.72*a^3/W^3-5.6*a^4/W^4}{(1-a/W)^{3/2}}$$

P_Q = *Applied load*

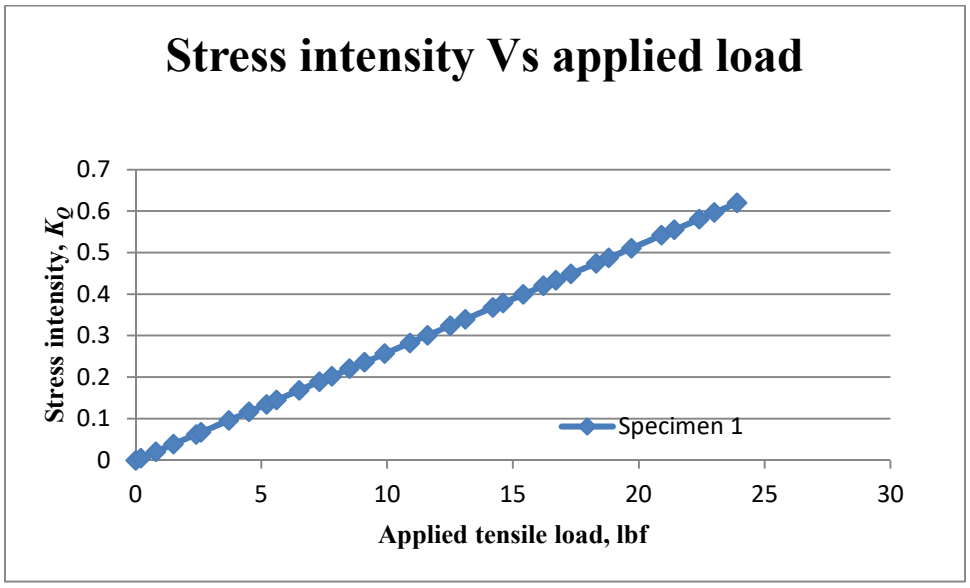

Figure 4.16: Determination of fracture toughness of PPS specimen 1

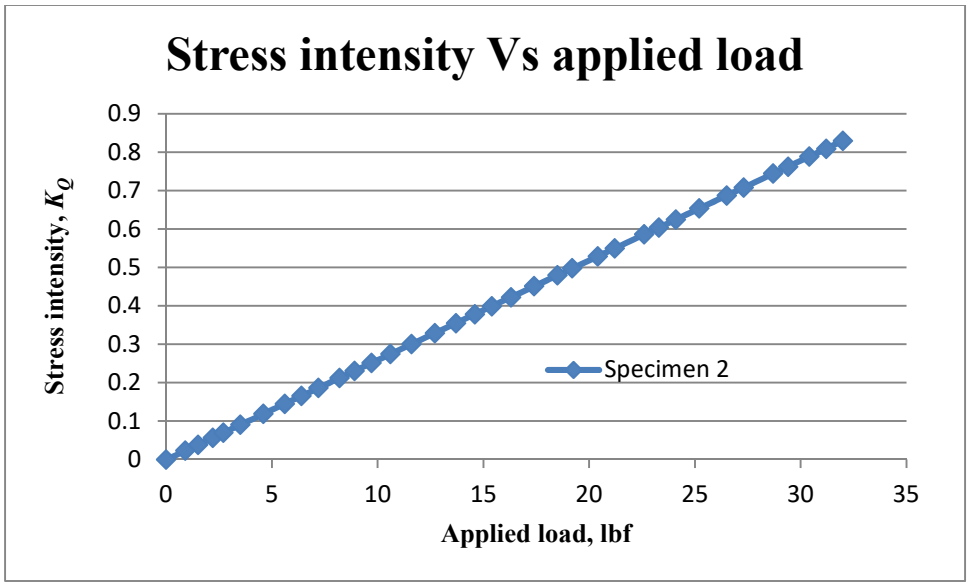

Figure 4.17: Determination of fracture toughness of PPS specimen 2

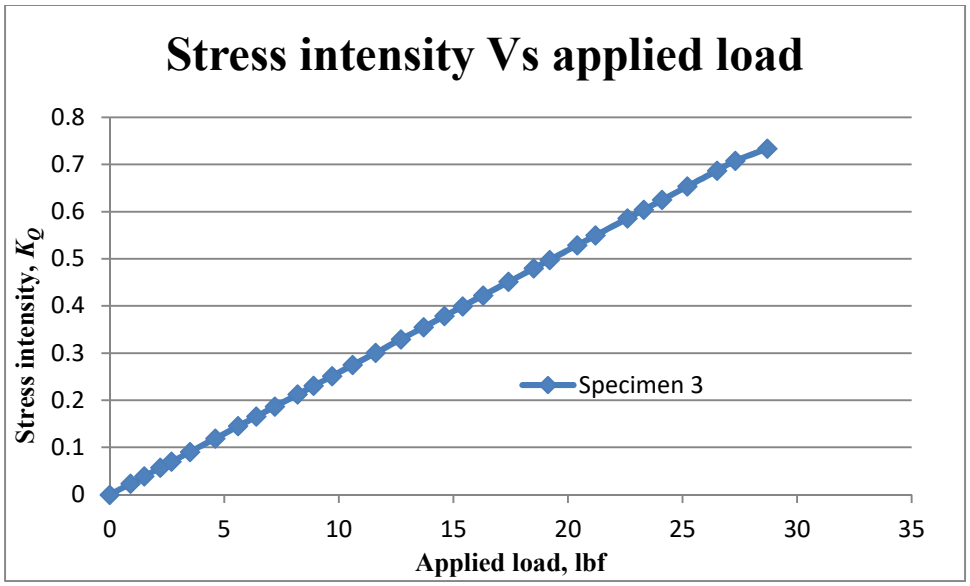

Figure 4.18: Determination of fracture toughness of PPS specimen 3

After averaging three values of fracture toughness of PPS, the final value was found as 0.725 MPa.m$^{0.5}$. At this point, all the welded samples were inspected using a digital optical microscope, and the notch lengths or un-welded lengths were determined. Using the fracture toughness and the crack length values, the residual strength or notched

tensile strength of the PPS samples was calculated according to equation (3). The joint efficiency was calculated as following:

$$Joint\ Efficiency\ = \frac{Notched\ Tensile\ Str\quad h}{Residual\ Tensile\ Strength}\ x\ 100\%$$

The results are listed in Table 4.6.

Table 4.6: Joint efficiency of the welded samples

Trial no	*Notched Strength of Welded Specimen (MPa)*	*Experimental K_{IC} ($MPa.m^2$)*	*a (mm)*	*Piecewise Residual Strength, (MPa)*	*Joint Efficiency (%)*
1	*9.85*	*0.725*	*0.91*	*12.11*	*81.3*
2	*2.87*	*0.725*	*0.70*	*13.80*	*20.8*
3	*1.10*	*0.725*	*1.50*	*9.43*	*12.1*
4	*9.51*	*0.725*	*1.00*	*11.55*	*82.3*
5	*6.21*	*0.725*	*0.75*	*13.34*	*46.5*
6	*9.41*	*0.725*	*1.00*	*11.55*	*81.4*
7	*6.63*	*0.725*	*1.25*	*10.33*	*64.1*
8	*3.94*	*0.725*	*0.75*	*13.34*	*29.5*
9	*10.17*	*0.725*	*0.89*	*12.24*	*83.0*
10	*2.23*	*0.725*	*0.66*	*14.22*	*15.7*
11	*9.65*	*0.725*	*0.94*	*11.91*	*81.0*
12	*9.15*	*0.725*	*1.00*	*11.55*	*79.2*
13	*4.88*	*0.725*	*1.00*	*11.55*	*42.2*
14	*3.86*	*0.725*	*1.00*	*11.55*	*33.4*
15	*4.25*	*0.725*	*1.20*	*10.54*	*40.3*
16	*3.76*	*0.725*	*1.00*	*11.55*	*32.5*
17	*7.31*	*0.725*	*1.30*	*10.13*	*72.1*
18	*2.54*	*0.725*	*1.00*	*11.55*	*21.9*

It is notable that trial no 1, 4, 6, 9 and 11 yielded more than 80% of the fracture toughness strength. Therefore, the combination of welding parameters for

these trials are the most effective compared to other combinations. It is also noted that the notched tensile strength of trial 9 is higher than that of trial 4, and the joint efficiency of trial 9 is also greater than the joint efficiency of trial 4.

4.4.6 Friction stir welding with stationary shoulder arrangement

A stationary shoulder arrangement as described in experimental setup 2 was used to weld PPS sample. When compared to the rotating shoulder, friction between the stationary shoulder and the specimen was reduced. In total 2 specimens were welded and tested under tensile loading condition. The welding parameters in this case were as follows:

Material temperature	: 80°C
Heating duration	: 10 min
Rotational speed	: 675 rpm
Traverse speed	: 2 mm/min

While working with rotating shoulder arrangement, the parameters mentioned above yielded maximum joint efficiency. It was found from this experiment that the top surface finishing of the joints was smooth, and the residual strength of the joints was consistent with the rotating shoulder arrangement. Figure 4.19 shows one of the specimens welded with the stationary shoulder and Table 4.7 shows the joint efficiency of the welded samples. It can be noted that the joint efficiency is more than 80% of the residual tensile strengths of PPS.

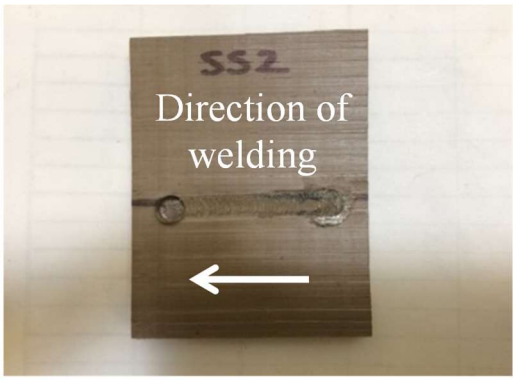

Figure 4.19: Specimen made using stationary shoulder

Table 4.7: Experimental results with stationary shoulder

Specimen ID	*Notched Strength of Welded Specimen (MPa)*	*Experimental K_{IC} ($MPa.m^{0.5}$)*	*a (mm)*	*Piece wise Residual Strength, (MPa)*	*Joint Efficiency (%)*
A	*10.01*	*0.725*	*0.90*	*12.33*	*82.49*
B	*15.54*	*0.725*	*0.37*	*18.98*	*81.85*

4.4.7 Comparison of un-notched tensile strengths

Tensile strength of un-notched pure PPS sample was determined using ASTM D638 standard. Using this standard, three identical test specimens were prepared as per type I specimen dimension. After averaging three values of tensile strengths of unreinforced PPS, the final tensile strength was found as 53.72 MPa.

It was observed that the notched tensile strengths of welded PPS samples were higher with stationary shoulder arrangement with welding parameters of HD10MT80RS675TS2. Therefore, two samples were prepared using these parameters and the un-welded sections were machined off using electric sander. Using ASTM D638

standard, tensile strengths were calculated. Table 4.8 shows the comparison of the tensile strengths. It is noted that the notch removed tensile strengths of the PPS samples are close to 80% of the base tensile strength.

Table 4.8: Comparison of notch removed tensile strength of PPS samples with un-notched tensile strength

Specimen ID	Notch Removed Tensile Strength, MPa	Base Material Tensile Strength, MPa	% of Base Strength
TS1	40.25	53.72	74.93
TS2	42.06	53.72	78.29

CHAPTER 5

INVESTIGATION OF FRICTION STIR WELDING OF CARBON FIBER REINFORCED PEEK.

5.1 Background

Polyetheretherketone (PEEK) is a high performance semi-crystalline thermoplastic polymer which has an excellent property profile. It has a relatively high melting point (about 350°C) compared to PPS with the advantages of easy process-ability by injection molding and other techniques that are common to thermoplastic polymers. As with other thermoplastics the addition of short fibers makes it effective in its ability to influence certain material properties such as friction and wear behavior. It has a highly stable chemical structure, which gives it an edge over other materials [44].

5.2 Determination of Thermal Properties of PEEK

In this study, 30% carbon fiber reinforced extruded PEEK plates were used for butt joining process. These plates were supplied by Quantum polymers. The carbon fibers in these plates were short and randomly oriented. The glass transition temperature (T_g) and the melting point (T_m) of PEEK samples were determined using Differential Scanning Calorimetry. The samples were prepared from the plates as received, and their weights were measured. The start temperature in DSC analysis was 30 °C and the samples were heated up to 400 °C with a heat rate of 20 °C /min. The samples were then cooled down to 30 °C with a heat rate of 50 °C /min. The lowest T_g of PEEK was found

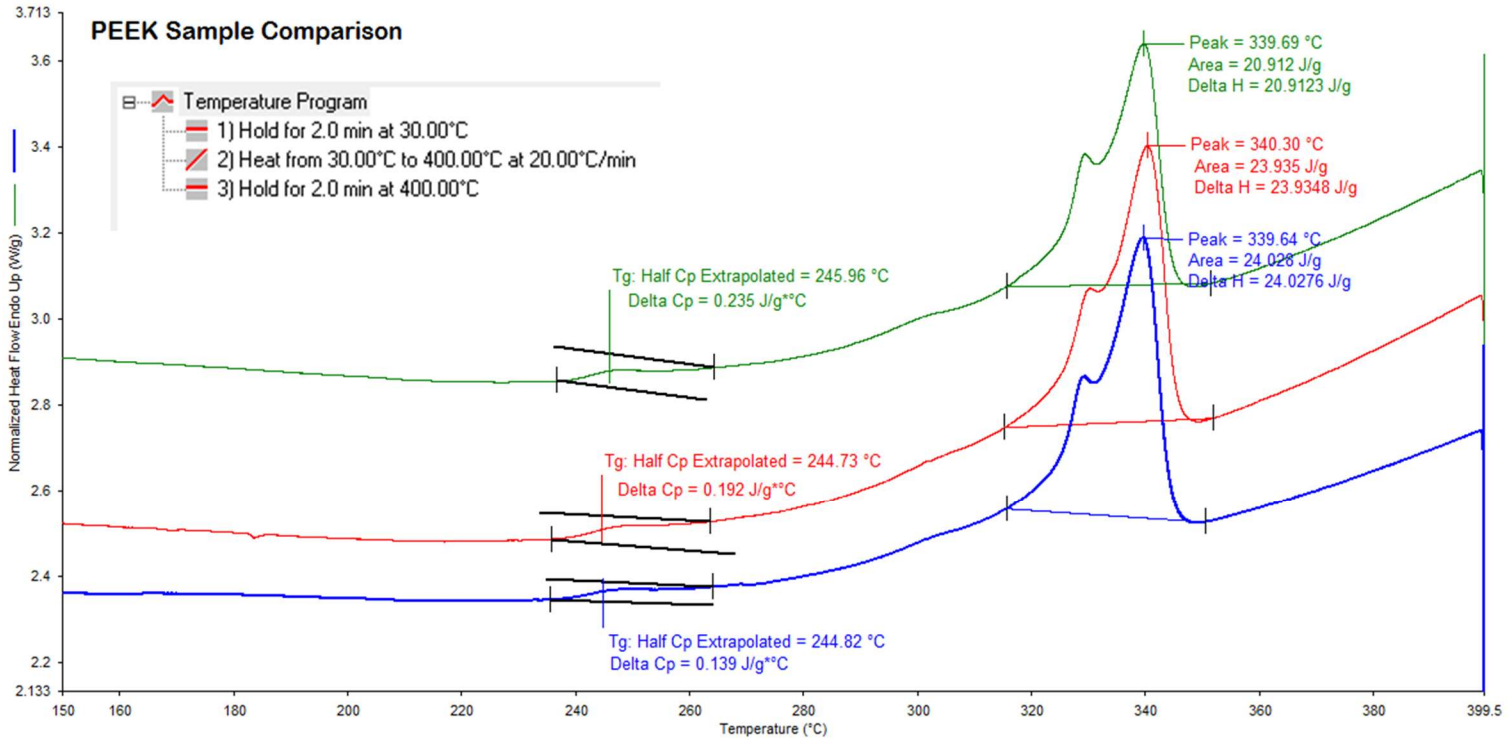

Figure 5.1: Determination of glass transition temperature and melting point of PEEK using DSC

as 244.82 °C and the average temperature of three samples was 245.17 °C. On the other hand, the average melting point of the PEEK sample was determined as 340 °C. The results obtained from DSC are presented in Figure 5.1.

5.3 Experimental Method

To investigate the friction stir weldability of carbon fiber reinforced PEEK, material temperature, tool rotational speed and tool traverse speed were taken as welding parameters. The heating duration for this investigation was 10 minutes after stabilization of bottom surface temperature. A stationary shoulder was employed during the welding phase. Before starting the actual welding, all the specimens were preheated from their bottom surface with a surface heater. Dimensions of the test specimen were the same as the PPS test specimen that are shown in Figure 4.3.

Table 5.1: Welding parameters for PEEK samples

Welding Parameters	*Level 1*	*Level 2*	*Level 3*	*Level 4*
Bottom surface Temperature (°C)	*210*	*310*	--	--
Tool Traverse Speed (mm/min)	*25*	*50*	*75*	--
Tool Rotational Speed (RPM)	*700*	*800*	*900*	*1000*

5.4 Experimental Design

Two levels of material bottom surface temperature were considered in this investigation. These were 310°C and 210°C. Beyond 310°C, melting of PEEK resin was observed. On the other hand, below 210°C, the quality of welded joint was poor.

Specimen thickness ranged from 4 mm to 5mm. Depending on the thickness, material top surface temperature was ranged from 195°C to 225°C. Parameters such as tool rotational speed and tool traverse speed were also varied in such a way that produced smooth weld surfaces. Table 5.1 provides all the welding parameters with their variations. All these parameters were identified through experiments until reliable welded joints were found. It can be noted that the traverse speed is much higher than that of PPS samples due to the ductile nature of PEEK resin.

5.5 Results and Discussion

Using friction stir welding parameters as stated in Table 5.1, 24 trials were performed. During these trials, there was a temperature difference between the bottom surface and the top surface of each sample. Due to this difference in temperature, bottom surface of each sample was expanded more than the top surface. This uneven material expansion resulted in some degree of bending of each sample. The samples with these bends are illustrated in Figure 5.2.

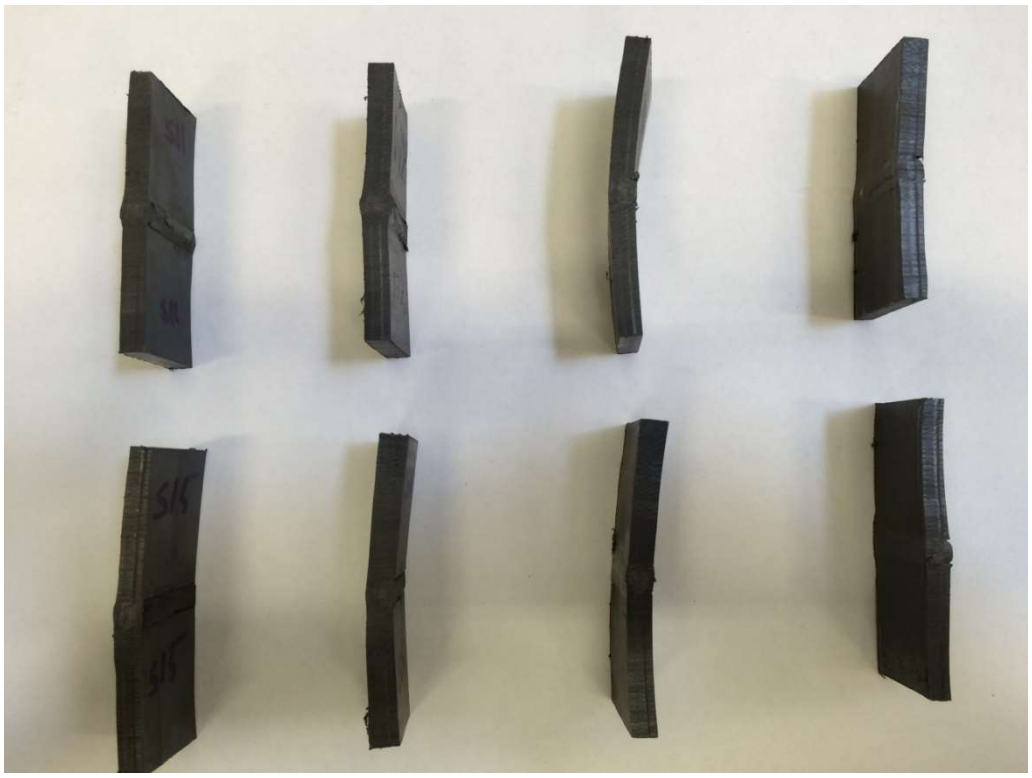

Figure 5.2: Welded samples with uneven material expansion

5.5.1 Surface morphology

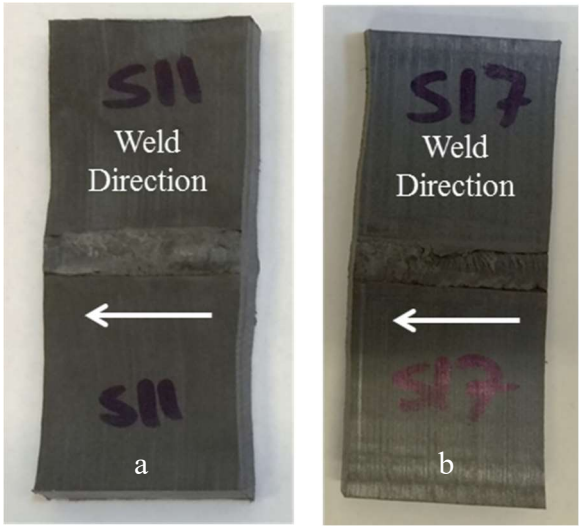

Figure 5.3: Snapshot of welded PEEK samples with welding parameters: (a) 900 rpm and 50 mm/min (b) 1000 rpm and 75 mm/min

5.5.2 Determination of notched tensile strength

Similar to PPS samples, PEEK samples had unwelded section close to the bottom of each sample. While determining tensile stresses, these unwelded sections acted as cracks or notches. Tensile tests were performed using ASTM D638 standard considering these notches. Test results and corresponding welding parameters are shown in Table 5.4.

Table 5.2: Notched tensile test results with varying welding parameters

Sample ID	*Material Temperature, °C*	*Tool Rotational Speed, rpm*	*Tool Traverse Speed, mm/min*	*Notched Tensile Strength, MPa*
A	*310*	*700*	*50*	*24.88*
B	*310*	*800*	*25*	*37.52*
C	*310*	*800*	*50*	*17.66*
D	*310*	*900*	*50*	*43.81*
E	*310*	*1000*	*50*	*35.81*
F	*310*	*1000*	*75*	*21.62*

5.5.3 Comparison of notched tensile strength with remaining strength

To determine the remaining strength, fracture toughness of PEEK samples were measured. Using the dimensions stated in Figure 4.14and Figure 4.15, identical test specimens of PEEK samples were prepared. Using MTS, these specimens were tested under tensile force, where the speed of testing was 5 mm/min. The displacement and corresponding tensile loads were recorded for each of the samples. Dimensions of each specimen are stated in Table 5.3.

Table 5.3: Specifications of PEEK samples for K_{IC} testing

Value of B, mm	*Value of B, cm*	*Value of W, mm*	*Value of W, cm*	*Value of a, cm*	*a/w*	*f(a/W)*
11	*1.1*	*22*	*2.2*	*1.1*	*0.5*	*9.517657*

The stress intensity, K_Q was calculated using following equation:

$$K_Q = (P_Q/BW^{1/2}) * f(a/W)$$

Where,

$$f(a/W) = \frac{\left(2+\frac{a}{W}\right)*(0.866+4.6a*\frac{a}{w}-13.32*a^2/W^2+14.72*a^3/W^3-5.6*a^4/W^4}{(1-a/W)^{3/2}}$$

P_Q = *Applied load*

The highest value of the stress intensity, K_Q where the specimen fractures is the fracture toughness of the specimen. Figure 5.4, Figure 5.5 and Figure 5.6show the variation of fracture toughness as the load increases on specimen 1 and specimen 2 respectively.

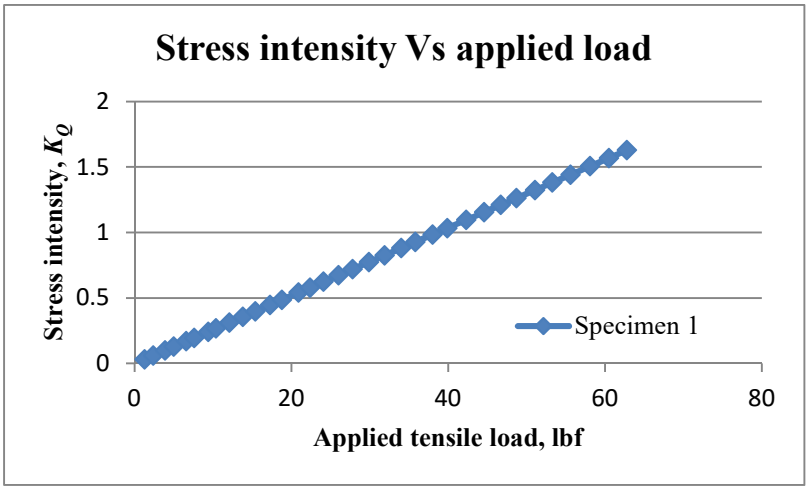

Figure 5.4: Determination of fracture toughness of specimen 1.

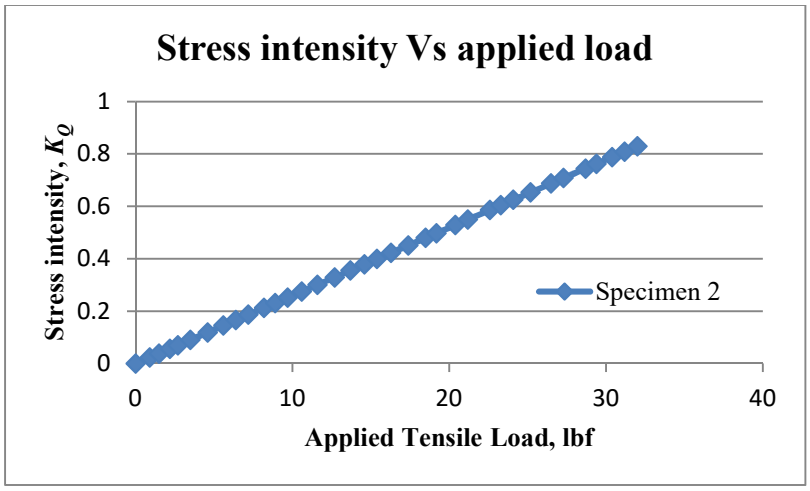

Figure 5.5: Determination of fracture toughness of specimen 2

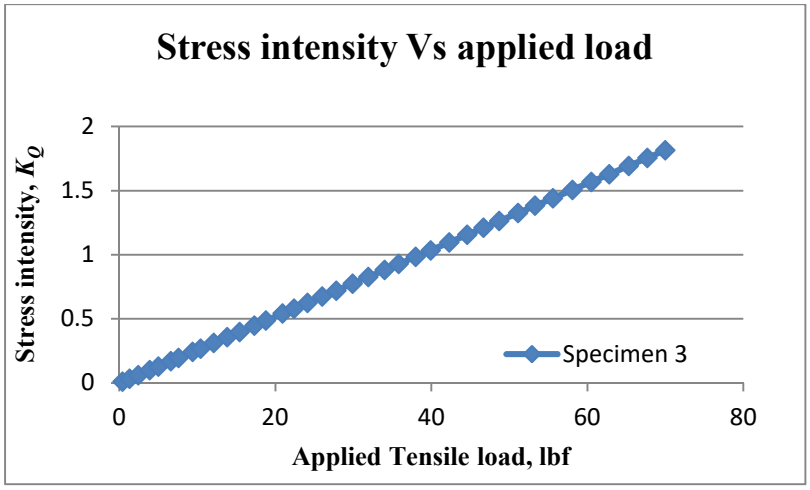

Figure 5.6: Determination of fracture toughness of specimen 2

Thus, the average value of K_{IC} of PEEK samples was determined as 1.43 MPa.m$^{0.5}$. Using optical microscope, lengths of the un-welded segment of each welded specimen were determined. At this point, using equation (3), the remaining tensile strength corresponding to each test sample was calculated. Final results are shown in Table 5.4.

Table 5.4: Comparison of notched tensile strength with residual tensile strength.

Specimen ID	*Notched Tensile Strength (MPa)*	*Experimental K_{IC} ($MPa.m^{0.5}$)*	*Notch Length, a (mm)*	*Residual Tensile Strength (MPa)*	*Joint Efficiency (%)*
A	*24.88*	*1.43*	*0.51*	*31.90*	*78.00*
B	*37.52*	*1.43*	*0.26*	*44.67*	*83.99*
C	*17.66*	*1.43*	*1.10*	*21.72*	*81.31*
D	*43.81*	*1.43*	*0.20*	*50.94*	*86.01*
E	*35.81*	*1.43*	*0.29*	*42.30*	*84.66*
F	*21.62*	*1.43*	*0.76*	*26.13*	*82.74*

It can be seen from Table 5.4 that the sample D has the largest residual tensile strength and the largest joint efficiency. Sample D also has the largest notched tensile strength. Table 5.4 also shows that sample B and sample E have similar notched tensile strength (37.52 MPa and 35.81 MPa) and joint efficiency (83.99% and 84.66%). Therefore, it can be said that the variations of tool rotational speed and tool traverse speed are negligible on these samples. While sample C and sample F have relatively lower notched tensile strength compared to sample B and E, the joint efficiencies of sample C and F are close to that of sample B and E.

5.5.4 Comparison of notch removed tensile strength with un-notched tensile strength

To determine the un-notched tensile strength of 30% carbon fiber reinforced PEEK, ASTM D638 standard was followed. According to this standard, Type-I sample dimension was chosen as the thickness of the PEEK samples were below 7mm. Using MTS, tensile strengths of three identical specimen were determined. The average un-notched tensile strength of PEEK samples was 116 MPa.

Figure 5.7: Tensile test arrangement of PEEK samples using MTS

Figure 5.8: Tensile test specimen after fracture

Two new welded samples were prepared using the welding parameters designed for sample D and E. The un-welded sections were machined off carefully using electric sander. The next step was to determine the tensile strengths of these samples using MTS. In Table 5.5, the notch removed tensile strengths of the PEEK samples were compared with un-notched tensile strength. It is notable that the maximum tensile strength is about 73% of un-notched tensile strength.

Table 5.5: Comparison of notch removed tensile strength with un-notched tensile strength

Specimen ID	*Notch removed Tensile Strength, MPa*	*Un-notched Tensile Strength, MPa*	*Ratio (%)*
T1D	*85.63*	*116.6*	*73.44*
T2E	*77.13*	*116.6*	*66.15*

5.5.5 Investigation of Failure of PEEK samples

Fracture analysis

In these experiments, the length of un-welded section was kept as small as possible by taking the tool length equal to test specimen thickness. However, during welding, void lines appeared in specimen C and F at the interphase of joint lines and the base material. During tensile test procedure, it was found that these void lines resulted into crack initiation, and failure occurred along these lines. Figure 5.9 shows the void line along where specimen C failed. In general, it was found that the void lines consist of absence of adequate material which in turn weakens the bonding between the stirred material and the base material. This weakening results into low tensile strength of the welded parts.

Figure 5.9: Failure of welded sample at the weld interphase.

5.5.6 Microstructures of PEEK samples

In case of carbon fiber reinforced PEEK, microstructures of the welded samples and that of the base material were compared using a digital optical microscope and a Scanning Acoustic Microscope (SAM). Welding parameters of the test specimen for which the micrographs were prepared were as follows:

Material bottom surface temperature : 210°C

Tool rotational speed : 800 rpm

Tool traverse speed : 25 mm/min

Heating Duration : 10 minutes

After completion of the welding, the sample was prepared for micrographs using a circular grinder and a polishing machine. The optical microscope was adjusted to get a magnification of 1000X.

Figure 5.10 and Figure 5.11 show a welded specimen and a base material using the optical microscope. In these two images, harder materials such as carbon fibers are seen white because they reflect more light than softer material such as PEEK resin.

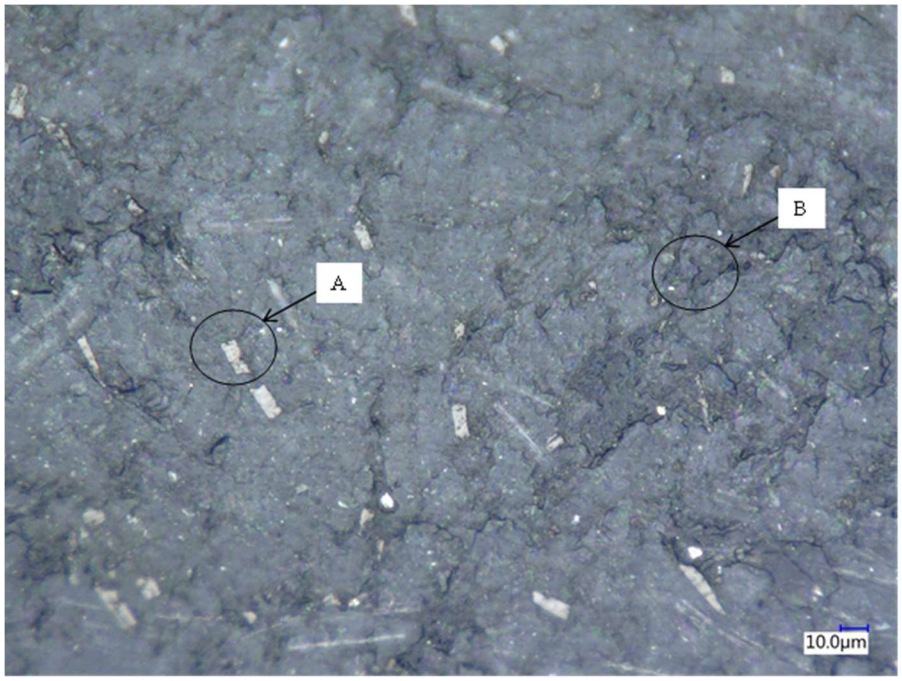

Figure 5.10: Micrograph at the joint line with 1000X magnification. Randomly oriented harder material (carbon fiber) seems white (A) embedded in soft PEEK matrix. The presence of cracks or void lines (B) are also visible.

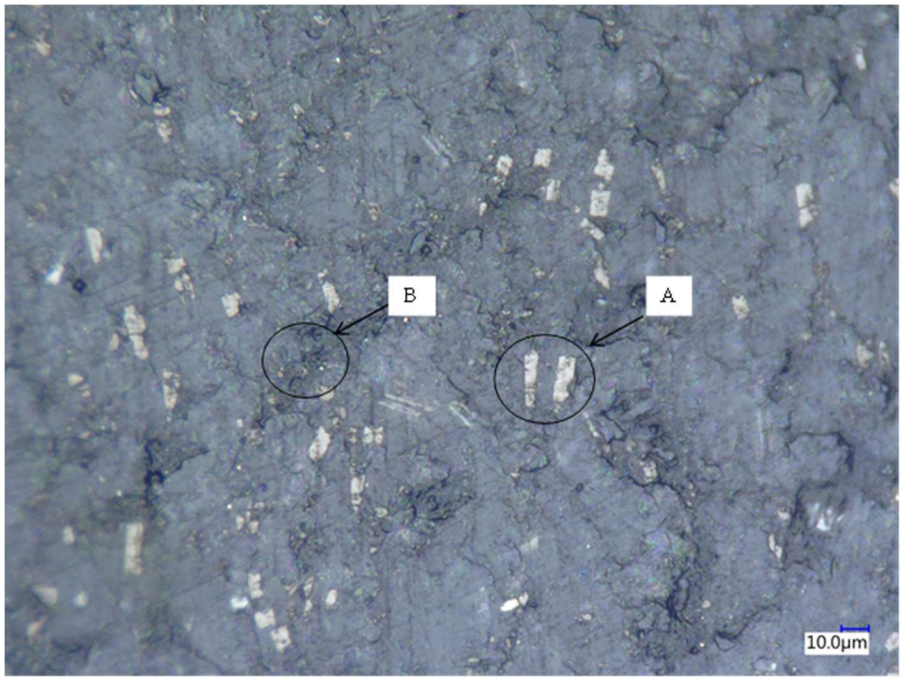

Figure 5.11: Micrograph at the base material away from weld zone with 1000X magnification. Randomly oriented carbon fiber seems white (A) embedded in soft PEEK matrix. Cracks or void lines (B) are lesser than the weld line.

Comparing these two images it was found that the base material had much less cracks and surface irregularities than the welded samples. However, voids are not visible with the help of these images, which can be observable by SAM. Figure 5.12 and Figure 5.13 show the images taken with SAM. In a SAM, ultrasonic waves were produced from a transducer and transported to the sample. After reflection, a receiver measures the amplitude, phase and elapsed time of the ultrasonic sound. Dense material section reflects sounds much better than a low dense section. In these two images, black spots are voids, which do not reflect sound waves. Solid bright lines are the mixture of carbon fibers and PEEK resin that reflects sound waves that are orthogonal to the upper surface of the samples.

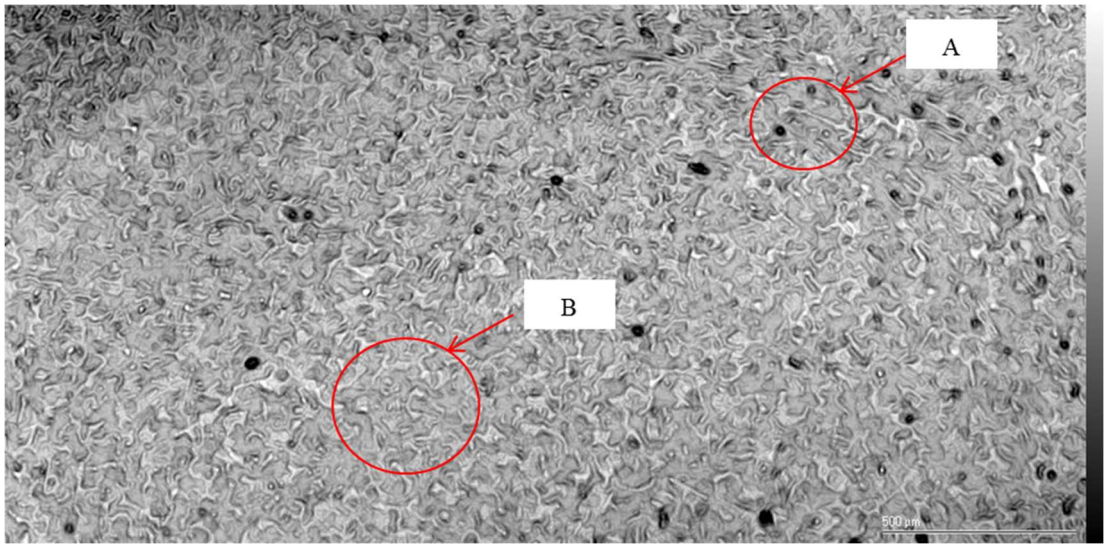

Figure 5.12: Micrograph at the weld location. Black spots (A) are voids on the surface of PEEK resin. Uniformly distributed carbon fibers (B) are also visible.

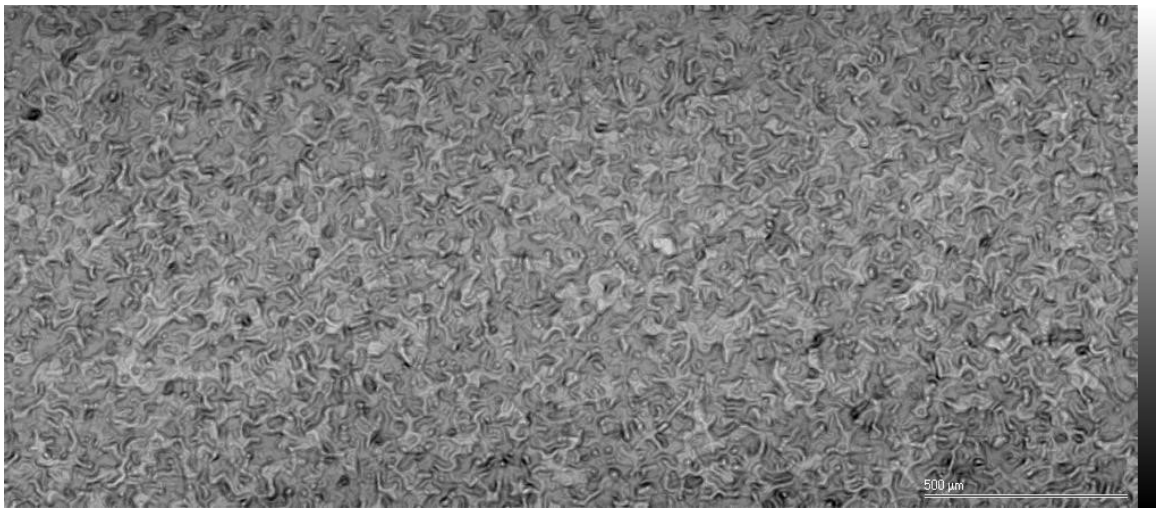

Figure 5.13: Micrograph at the base material away from the weld line. It has uniform texture and less voids.

It is seen from the micrograph that the welded section of the specimen has uniform distribution of PEEK resin and carbon fibers with some voids and micro cracks. On the other hand, the base material does not have voids and cracks in comparison with the welded material. It can be concluded that the increased presence of voids and micro-

cracks in welded sample can be one of the reasons for lower tensile strength than the base material.

CHAPTER 6

CONCLUSIONS AND FUTURE WORKS

6.1 Conclusions

Preliminary FSW process development work has been done for two thermoplastic materials – unreinforced PPS and short carbon fiber reinforced PEEK. Based on the analytical models for the heat generation in FSW process and experimental results, it was found that only tool rotational speed was not sufficient to produce enough heat to weld these two thermoplastic materials. This led to the addition of external heat sources in the welding process.

An external heat source, a strip heater, was placed at the bottom of two identical weld pieces. During the course of experiments, heating intensity was varied. Other process parameters, tool rotational speed and tool transverse speed, were also varied in addition to material temperature. From initial experiments, welded joints were found and a range of process variables were identified. Using Taguchi's design of experiment method, output characteristic of FSW process such as tensile strength was evaluated for PPS, and optimum configuration of process variables were determined. It was also found that increasing tool traverse speed lowers the notched tensile strength of PPS joint. Rotating and stationary shoulder arrangements were utilized to weld PPS samples. The maximum notched removed tensile strength of PPS samples was found close to 80% of the base tensile strength.

Short carbon fiber reinforced PEEK samples were welded with a higher traverse speed in compared to PPS sample. In this study, a joint strength of 77.13 MPa was achieved for PEEK samples with a traverse speed of 50 mm/min. Due to the setup of the experiments, an un-welded section was present in the samples, which act as a crack or notch during tensile tests. The fracture toughness tests were performed for both PPS and PEEK samples to observe the influence of un-welded segments in the workpiece cross section at the weld. The notched tensile strengths of the welded parts were compared with the remaining strengths of the samples. It was found that the presence of un-welded lengths significantly influence its un-notched tensile strength. For PEEK samples, fracture pattern and micrograph at the weld line was studied. It was observed that the cracks and voids were present at the interphase between the advancing or retreating side of the welded samples.

6.2 Future Work

In this work, the friction stir welding method was utilized to join unreinforced PPS and short carbon fiber reinforced PEEK. In the past, researchers worked on joining different polymers other than PPS and PEEK using this welding technique. But most of them were limited to friction stir spot welding. This new method will allow us to choose the welding parameters to join the PPS and PEEK. Further research on FSW of unreinforced PPS and reinforced PEEK should focus on

(1) Determination of friction coefficients and contact pressure: to determine the friction co-efficient, a tribological study can be conducted to determine the surface quality of the FSW tool and the material to be joined. On the other hand, to determine the

pressure between the FSW tool and the material, the force applied parallel to the axis of rotation of the tool or the downward force can be measured.

(2) Optimization of process parameters to maximize the weld strength: all the process parameters including contact pressure can be studied further to optimize the joint strength. Tool geometry has an enormous effect on the joint strength. Therefore, this can also be varied during the optimization process.

(3) Application of optimized process parameters to get other types joint: other types of joints such as corner joint and 'T' joint can be developed with the help of friction stir welding.

(4) Heat generation process development: a large extent of work can be emphasized on the heat generation process. In addition to resistance type surface heater, feasibility of using induction heating and infrared heating can be studied.

(5) Measurement of torque and force: to get a better control over the combination of the welding parameters, the torque and force applied to the weld piece during the welding phase can be measured. The measurement of x-directional and y-directional force applied by the FSW tool can be studied to improve the joint quality.

(6) Development of further joining configuration: in addition to simple butt joining configuration, other joining configuration can be investigated using the process described in this study. A study on 'Tee' joint configuration with continuous fiber thermoplastics can be performed by adding an unreinforced support element at the joint line.

(7) Investigation of thermoplastic and metal joining process: this study can be further extended to the investigation of thermoplastic and metal joining process.

REFERENCES

[1] T. Dubois, "Thermoplastics Eyed As Alternative For Metals," Aviation Week & Space Technology, Sep 1, 2014.

[2] S. Black, "High-Performance Composites," 4 March 2014. [Online]. Available: http://www.compositesworld.com/articles/thermoplastic-composites-save-weight-in-rotorcraft-aerostructure. [Accessed 1 July 2016].

[3] F. George, "Latest Business Jet Offering Raises The Bar," Aviation Week & Space Technology , March 25, 2013.

[4] A. Yousefpour, M. Hojjati and J. Immarigeon, "Fusion Bonding/Welding of Thermoplastic Composites," *Journal of Thermoplastic Composite Materials,* vol. 17, pp. 303-341, 2004.

[5] A. Weber, "Composite Joining: Fastener Pros and Cons," *Assembly Magazine,* 2 May 2013.

[6] C. Ageorges, L. Ye and M. Hou, "Advances in fusion bonding techniques for joining thermoplastic matrix composites: a review," *Composites:Part A,* vol. 32, pp. 839-857, 2001.

[7] B. Gibson, D. Lammlein, T. Prater, W. Longhurst, C. Cox, M. Ballun, K. Dharmaraj, G. Cook and A. Strauss, "Friction stir welding: Process, automation, and control," *Journal of Manufacturing Processes,* vol. 16, pp. 56-73, 2014.

[8] S. Hoseinlaghab, S. Mirjavadi, N. Sadeghian, I. Jalili, M. Azarbarmas and M. Givi, "Influences of welding parameters on the quality and creep properties of friction stir welded polyethylene plates," *Materials & Design,* vol. 67, pp. 369-378, 2015.

[9] A. Bagheri, T. Azdast and A. Doniavi, "An experimental study on mechanical properties of friction stir welded ABS sheets," *Materials and Design,* vol. 43, pp. 402-409, 2013.

[10] K. Panneerselvam and K. Lenin, "Joining of Nylon 6 plate by friction stir welding process using threaded pin profile," *Materials and Design,* vol. 53, pp. 302-307, 2014.

[11] "TWI Ltd.," The Welding Institute, [Online]. Available: http://www.twi-global.com/technologies/welding-surface-engineering-and-material-processing/friction-stir-welding/benefits-and-advantages/. [Accessed 15 December 2014].

[12] N. Mendes, A. Loureiro, C. Martins, P. Neto and J. Pires, "Morphology and strength of acrylonitrile butadiene styrene welds performed by robotic friction stir welding," *Materials and Design,* vol. 64, pp. 81-90, 2014.

[13] E. Cerri and P. Leo, "Warm and room temperature deformation of friction stir welded thin aluminium sheets," *Materials & Design,* pp. 1392-1402, 2010.

[14] A. Paoletti, F. Lambiase and A. Di Ilio, "Optimization of friction stir welding of thermoplastics," in *Procedia CIRP ICME '14*, Capri (Naples), Italy, 2014.

[15] M. K. Bilici, "Application of Taguchi approach to optimize friction stir spot welding parameters of polypropylene," *Materials and Design,* vol. 35, pp. 113-119, 2012.

[16] W. Li, T. Fu, L. Hilgert, J. Hilgert, F. Wang, J. dos Santos and N. Huber, "Effects of tool rotational and welding speed on microstructure and mechanical properties of bobbin-tool friction-stir welded Mg AZ31," *Materials & Design,* vol. 64, pp. 714-720, December 2014.

[17] Y. Zhao, Z. Lu, K. Yan and L. Huang, "Microstructural characterizations and mechanical properties in underwater friction stir welding of aluminum and magnesium dissimilar alloys," *Materials & Design,* vol. 65, pp. 675-681, 2015.

[18] S. R. Strand, C. D. Sorensen and T. W. Nelson, "Effects of friction stir welding on polymer microstructure," in *ANTEC 2003*, Nashville, May 2003.

[19] M. Pirizadeh, T. Azdast, S. R. Ahmadi, S. M. Shishavan and A. Bagheri, "Friction stir welding of thermoplastics using a newly designed tool," *Materials and Design,* vol. 54, pp. 342-347, 2014.

[20] S. Saeedy and M. Givi, "Investigation of the effects of critical process parameters of friction stir welding of polyethyleneg," *Journal of Engineering Manufacture,* vol. 225 (B), pp. 1305-1310, 2010.

[21] A. Arici and T. Sinmaz, "Effects of double passes of the tool on friction stir welding of polyethylene," *Journal of Materials Science,* vol. 40, pp. 3313-3316, 2005.

[22] E. Squeo, G. Bruno, A. Guglielmotti and F. Quadrini, "Friction stir welding of polyethylene sheets," *The Annals of Dunarea de Jos University of Galati, Technologies in Machine Building,* vol. 5, pp. 241-246, 2009.

[23] M. Djurdjanović, M. Mijajlović, D. Milčić and D. Stamenković, "Heat Generation During Friction Stir Welding Process.," *Tribology in Industry,* Vols. 31(1-2), pp. 8-14, 2009.

[24] J. Arbegast, "Friction stir welding after a decade of development," *Welding Journal,* vol. 85, no. 3, March 2006.

[25] P. L. Threadgill, "Terminology in friction stir welding," *Science and Technology of Welding and Joining,* pp. 357-360, 2007.

[26] P. Colegrove, M. Pinter, D. Graham and T. Miller, "Three Dimensional Flow and Thermal Modeling of the Friction Stir Welding Process," in *Proceedings of the Second International Symposium on Friction Stir Welding*, Gothenburg, Sweden, June 26-28,2000.

[27] X. Lui, S. Lan and J. Ni, "Analysis of process parameters effects on friction stir welding of dissimilar aluminum alloy to advanced high strength steel," *Materials & Design,* vol. 59, pp. 50-62, July 2014.

[28] J. Guo, H. Chen, C. Sun, G. Bi, Z. Sun and J. Wei, "Friction stir welding of dissimilar materials between AA6061 and AA7075 Al alloys effects of process parameters," *Materials & Design,* vol. 56, pp. 185-192, April 2014.

[29] P. Biswas and N. Mandal, "Effect of Tool Geometry on Thermal History of FSW of AA1100," *Welding Journal,* vol. 90, pp. 129-135, 2011.

[30] C. A. Maltin, L. J. Nolton, J. L. Scott, A. I. Toumpis and A. M. Galloway, "The potential adaptation of stationary shoulder friction stir welding technology to steel," *Materials & Design,* vol. 64, pp. 614-624, December 2014.

[31] J. Maxwell, Theory of Heat, Dover Publications, Inc., 1871.

[32] B. Mills-Dadson, A. I. Islam, K. Asamene and M. Sundaresan, "Monitoring Friction Related Surface Degradation Using Acoustic Emission Technique," in *Proceedings of SPIE - The International Society for Optical Engineering (Proceedings of SPIE)*, 2013.

[33] H. Schmidt, J. Hattel and J. Wert, "An analytical model for the heat generation in friction stir welding," *Modelling and Simulation in Materials Science and Engineering,* vol. 12, pp. 143-157, 2004.

[34] H. Hira, H. Aoki and T. Shibayanagi, "Study on the friction stir welding bahavior of several thermoplastics," in *Proceedings of the 1st Ineternational Symposium on Joining and Welding*, Osaka, Japan, 2013.

[35] R. PJ., Taguchi techniques for quality engineering, New York: Mc-Graw Hill, 1988.

[36] G. Taguchi, S. Chowdhury and Y. Wu, Taguchi's Quality Engineering Handbook, Hoboken, New Jersey: John Wiley & Sons, 2005.

[37] M. S. Yagfarov and E. Mitrofanova, "Recrystallization and secondary crystallization in polymers," *Polymer Science,* vol. 28, no. 5, pp. 1011-1017, 1986.

[38] G. Peace, Taguchi methods., New York:Addison-Wesley, 1993.

[39] S. Juang and Y. Tarng, "Process parameter selection for optimizing the weld pool geometry in the inert gas welding of stainless steel," *Journal of Materials Processing Technology,* vol. 122, pp. 33-37, 2002.

[40] R. K. Roy, Design of Experiments Using The Taguchi Approach: 16 steps to product and process, New York: John Wiley & Sons, 2001.

[41] W. H. Yang and Y. S. Tarng, "Design optimization of cutting parameters for turning operations based on the Taguchi method," *Journal of Materials Processing Technology,* vol. 84, no. 1-3, pp. 122-129, 1998.

[42] J. M. Whitney and R. J. Nuismer, "Stress Fracture Criteria for Laminated Composites Containing Stress Concentrations," *Journal of Composite Materials,* vol. 8, no. 3, pp. 253-265, July 1974.

[43] J. Schijve, Fatigue of Structures and Materials, Springer Science & Business Media, Dec 16, 2008, p. 115.

[44] K. Friedrich, Z. Lu and R. Scherer, "Wear and Friction of Composite Materials," in *Proceedings of Symposium A4 on Composite Materials of International Conference on Advanced Materials-ICAM91*, Strasbourg, France, 1991.

[45] X. Peet, "Passing the value test, The Boeing technology advantage," The Boeing Company, 2006.

[46] A. Liu, Mechanics and Mechanisms of Fracture: An Introduction, Materials Park, OH: ASM International, 2005.

[47] Y. J. Chao, X. Qi and W. Tang, "Heat Transfer in Friction Stir Welding - Experimental and Numerical Studies," *Journal of Manufacturing Science and Engineering,* vol. 125, pp. 138-145, February 2003.

APPENDIX A

SAMPLE G-CODE

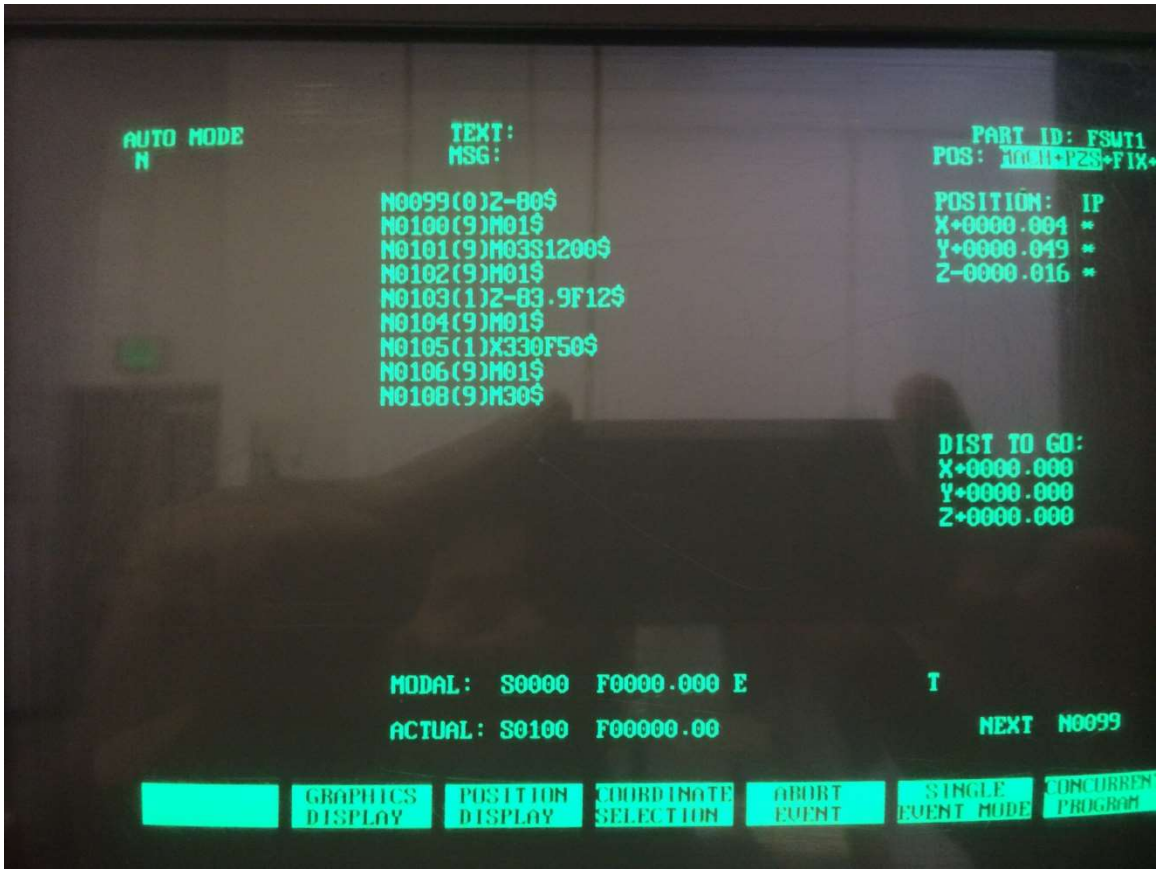

APPENDIX B

TABLE OF CRITICAL VALUES FOR THE F-DISTRIBUTION

Table of critical values for the F distribution (for use with ANOVA):

How to use this table:

There are two tables here. The first one gives critical values of F at the p = 0.05 level of significance. The second table gives critical values of F at the p = 0.01 level of significance.
1. Obtain your F-ratio. This has (x,y) degrees of freedom associated with it.
2. Go along x columns, and down y rows. The point of intersection is your critical F-ratio.
3. If your obtained value of F is equal to or larger than this critical F-value, then your result is significant at that level of probability.
An example: I obtain an F ratio of 3.96 with (2, 24) degrees of freedom.
I go along 2 columns and down 24 rows. The critical value of F is 3.40. My obtained F-ratio is larger than this, and so I conclude that my obtained F-ratio is likely to occur by chance with a p<.05.

Critical values of F for the 0.05 significance level:

	1	2	3	4	5	6	7	8	9	10
1	161.45	199.50	215.71	224.58	230.16	233.99	236.77	238.88	240.54	241.88
2	18.51	19.00	19.16	19.25	19.30	19.33	19.35	19.37	19.39	19.40
3	10.13	9.55	9.28	9.12	9.01	8.94	8.89	8.85	8.81	8.79
4	7.71	6.94	6.59	6.39	6.26	6.16	6.09	6.04	6.00	5.96
5	6.61	5.79	5.41	5.19	5.05	4.95	4.88	4.82	4.77	4.74
6	5.99	5.14	4.76	4.53	4.39	4.28	4.21	4.15	4.10	4.06
7	5.59	4.74	4.35	4.12	3.97	3.87	3.79	3.73	3.68	3.64
8	5.32	4.46	4.07	3.84	3.69	3.58	3.50	3.44	3.39	3.35
9	5.12	4.26	3.86	3.63	3.48	3.37	3.29	3.23	3.18	3.14
10	4.97	4.10	3.71	3.48	3.33	3.22	3.14	3.07	3.02	2.98
11	4.84	3.98	3.59	3.36	3.20	3.10	3.01	2.95	2.90	2.85
12	4.75	3.89	3.49	3.26	3.11	3.00	2.91	2.85	2.80	2.75
13	4.67	3.81	3.41	3.18	3.03	2.92	2.83	2.77	2.71	2.67
14	4.60	3.74	3.34	3.11	2.96	2.85	2.76	2.70	2.65	2.60
15	4.54	3.68	3.29	3.06	2.90	2.79	2.71	2.64	2.59	2.54
16	4.49	3.63	3.24	3.01	2.85	2.74	2.66	2.59	2.54	2.49
17	4.45	3.59	3.20	2.97	2.81	2.70	2.61	2.55	2.49	2.45
18	4.41	3.56	3.16	2.93	2.77	2.66	2.58	2.51	2.46	2.41
19	4.38	3.52	3.13	2.90	2.74	2.63	2.54	2.48	2.42	2.38
20	4.35	3.49	3.10	2.87	2.71	2.60	2.51	2.45	2.39	2.35
21	4.33	3.47	3.07	2.84	2.69	2.57	2.49	2.42	2.37	2.32
22	4.30	3.44	3.05	2.82	2.66	2.55	2.46	2.40	2.34	2.30
23	4.28	3.42	3.03	2.80	2.64	2.53	2.44	2.38	2.32	2.28
24	4.26	3.40	3.01	2.78	2.62	2.51	2.42	2.36	2.30	2.26
25	4.24	3.39	2.99	2.76	2.60	2.49	2.41	2.34	2.28	2.24
26	4.23	3.37	2.98	2.74	2.59	2.47	2.39	2.32	2.27	2.22
27	4.21	3.35	2.96	2.73	2.57	2.46	2.37	2.31	2.25	2.20
28	4.20	3.34	2.95	2.71	2.56	2.45	2.36	2.29	2.24	2.19
29	4.18	3.33	2.93	2.70	2.55	2.43	2.35	2.28	2.22	2.18
30	4.17	3.32	2.92	2.69	2.53	2.42	2.33	2.27	2.21	2.17
31	4.16	3.31	2.91	2.68	2.52	2.41	2.32	2.26	2.20	2.15
32	4.15	3.30	2.90	2.67	2.51	2.40	2.31	2.24	2.19	2.14
33	4.14	3.29	2.89	2.66	2.50	2.39	2.30	2.24	2.18	2.13
34	4.13	3.28	2.88	2.65	2.49	2.38	2.29	2.23	2.17	2.12
35	4.12	3.27	2.87	2.64	2.49	2.37	2.29	2.22	2.16	2.11